[Pt] 2 Pb Trinuclear Systems: Impact of the Anionic Platinum Fragment on the Lead Environment and Photoluminescence †

ARTICLE *in* INORGANIC CHEMISTRY · JULY 2008

Impact Factor: 4.76 · DOI: 10.1021/ic8006876 · Source: PubMed

Inorg. Chem. **2008**, *47*, 7703−7716

Inorganic Chemistry
Article

$[Pt]_2Pb$ Trinuclear Systems: Impact of the Anionic Platinum Fragment on the Lead Environment and Photoluminescence†

Jesús Rubén Berenguer,‡ Alvaro Díez,‡ Julio Fernández,‡ Juan Forniés,§ Ana García,‡ Belén Gil,‡ Elena Lalinde,*,‡ and M. Teresa Moreno‡

Departamento de Química-Grupo de Síntesis Química de La Rioja, UA-CSIC, Universidad de La Rioja, 26006, Logroño, Spain, and Departamento de Química Inorgánica, Instituto de Ciencia de Materiales de Aragón, Universidad de Zaragoza-Consejo Superior de Investigaciones Científicas, 50009 Zaragoza, Spain

Received April 17, 2008

A comparison of the solid structures of three novel trinuclear sandwich Pt_2Pb systems $(NBu_4)_2[\{Pt(C{\equiv}CTol)_4\}_2Pb(OH_2)_2]$ **1**, $[\{Pt(bzq)(C{\equiv}CPh)_2\}_2Pb]$ **2**, and $(NBu_4)[\{Pt(bzq)(C{\equiv}CC_6H_4{-}CF_3\text{-}4)_2\}_2Pb(O_2ClO_2)]$ **4** ($NBu_4[\mathbf{3}\cdot(O_2ClO_2)]$) with that of the previously reported $(NBu_4)_2[\{Pt(C_6F_5)_4\}_2Pb]$ **5** showed that the local environment of Pb^{II} is highly sensitive to the nature of the anionic platinate(II) precursors. The photoluminescence (PL) studies of all **1**−**5** complexes revealed a dependence of PL on the structure type. Thus, complexes **1** and **5** exhibit metal centered emissions (**1**, 497 nm, 77 K; **5**, 539 nm, $\phi = 0.43$, 298 K) related to the linear (**5**) or bent (**1** Pt−Pb−Pt 149.9°) trinuclear entities. However, in complexes **2**−**4**, that have unprecedented $Pb^{II}\cdots\eta^1(C{\equiv}CR)$ bonding interactions and very short Pt···Pb and Pt···Pt distances, the emissive state in solid state (77 K) is attributed to a ^{3}MLM′CT [Pt(1)π(C≡CR)→Pt(2)/Pb(sp)π^*(C≡CR)] state mixed with some $\pi\pi^*$ excimeric character in neutral complexes **2** (R = Ph) and **3** ($R = C_6H_4{-}CF_3$-4), and in the case of the adduct $(NBu_4)[\{Pt(bzq)(C{\equiv}CC_6H_4{-}CF_3\text{-}4)_2\}_2Pb(O_2ClO_2)]$ **4** modified also by $Pb^{II}\cdots O$ ($O_2ClO_2^-$) contacts.

Introduction

Luminescent mono and multinuclear complexes have attracted much recent research interest, primarily because of their potential applications in optoelectronic materials (sensors, light emitting diodes, artificial photosynthesis, etc.).[1–12] In this area, a great deal of research has been focused on alkynyl compounds, which have been shown to possess interesting photophysical properties.[12–24] In these systems, emissive manifolds depend on the metal and coligands and can also be elegantly fine-tuned by additional variations of the fragments and substituents on the carbon

† Dedicated to Professor Ernesto Carmona on the occasion of his 60th anniversary.

* To whom correspondence should be addressed. E-mail: elena.lalinde@unirioja.es.

‡ Universidad de La Rioja, UA-CSIC.

§ Universidad de Zaragoza-CSIC.

(1) Chou, P. T.; Chi, Y. *Chem.—Eur. J.* **2007**, *13*, 380.
(2) Cooke, M. W.; Hanan, G. S. *Chem. Soc. Rev.* **2007**, *36*, 1466.
(3) Evans, R. C.; Douglas, P.; Wiscom, C. J. *Coord. Chem. Rev.* **2006**, *250*, 2093.
(4) Holder, E.; Langeveld, B. M. W.; Schubert, U. S. *Adv. Mater.* **2005**, *17*, 1109.
(5) McClenaghan, M. D.; Leydet, N. D.; Maubert, Y.; Indelli, M. T.; Campagna, S. *Coord. Chem. Rev.* **2005**, *249*, 1336.
(6) Sun, S. S.; Lees, A. J. *Coord. Chem. Rev.* **2002**, *230*, 171.
(7) *Coord. Chem. Rev.* **2000**, *208* (Special Issue), 1−371.
(8) Wong, W. Y. *Comments Inorg. Chem.* **2005**, *26*, 39.
(9) Huynh, M. H. V.; Dattelbaum, D. M.; Meyer, T. J. *Coord. Chem. Rev.* **2005**, *249*, 457.
(10) Vogler, A.; Kunkely, H. *Top. Curr. Chem.* **2001**, *213*, 143.
(11) Thanasekaran, P.; Liao, R. T.; Liu, Y. H.; Rajendran, T.; Rajagopal, S.; Lu, K. L. *Coord. Chem. Rev.* **2005**, *249*, 1085.
(12) Yam, V. W. W. *C. R. Chim.* **2005**, *8*, 1194.
(13) Lai, S. W.; Chan, M. C. W.; Wang, Y.; Lam, H. W.; Peng, C. Y. *J. Organomet. Chem.* **2001**, *617*−*618*, 133.
(14) Wong, K. M. C. *Coord. Chem. Rev.* **2007**, *251*, 2400.
(15) Wong, K. M. C.; Yam, V. W. W. *Coord. Chem. Rev.* **2007**, *251*, 2477; and references therein.
(16) Castellano, F. N.; Pomestchenko, I. E.; Shikhova, E.; Hua, F.; Muro, M. L.; Rajapakse, N. *Coord. Chem. Rev.* **2006**, *250*, 1819.
(17) Yam, V. W. W. *J. Organomet. Chem.* **2004**, *689*, 1393.
(18) Yam, V. W. W.; Lo, W. Y.; Lam, C. H.; Fung, W. K. M.; Wong, K. M. C.; Lau, V. C. Y.; Zhu, N. *Coord. Chem. Rev.* **2003**, *245*, 39.
(19) Long, N. J.; Williams, C. K. *Angew. Chem., Int. Ed.* **2003**, *42*, 2586.
(20) Yam, V. W. W. *Acc. Chem. Res.* **2002**, *35*, 555.
(21) Slageren, J. V.; Klein, A.; Zalis, S. *Coord. Chem. Rev.* **2002**, *230*, 193.
(22) Puddephatt, R. J. *Coord. Chem. Rev.* **2001**, *216*−*217*, 313.
(23) Hissler, M.; McGarrah, J. E.; Connick, W. B.; Geiger, D. K.; Cummings, S. D.; Eisenberg, R. *Coord. Chem. Rev.* **2000**, *208*, 115.
(24) Ziessel, R.; Hissler, M.; El-ghayoury, A.; Harriman, A. *Coord. Chem. Rev.* **1998**, *178*−*180*, 1251.

10.1021/ic8006876 CCC: $40.75
Published on Web 07/15/2008

chain.[25–36] Furthermore, the alkynyl ligands exhibit a very good $\pi(\eta^2)$ coordinating capability, and we[37–45] and others[46–53] have demonstrated that the luminescence behavior is strongly influenced by perturbation of the electron density of the C≡C unit through $\eta^2\cdots$metal alkynyl bonding and also by metallophilic interactions.[37–53]

Homo and heteropolynuclear aggregates and clusters based on closed and/or subclosed-shell (d^8, d^{10}, $d^{10}s^2$) metallic interactions[54–58] have also been studied as interesting emitters.[59–73] The presence of strong metallophilic interactions determines their structures and is often cited as an essential factor of their remarkable photophysical properties.[54–57,59–73] The arrangement of the metals and, in particular, the type of metals and coligands have a profound effect on the photophysical behavior of the resulting polynuclear systems.[61,74] Therefore, the controlled formation of novel polymetallic systems of the above metals and the study of their structure property correlations are of great importance in designing functional materials. Within this field, compared to the numerous reports involving polar M-Tl[54,56,61,71,75–92]

(25) Li, X. L.; Dai, F. R.; Zang, L. Y.; Zhu, Y. M.; Peng, Q.; Chen, Z. N. *Organometallics* **2007**, *16*, 4483.
(26) Camerel, F.; Ziessel, R.; Donnio, B.; Bourgogne, C.; Guillon, D.; Schmutz, M.; Iacovita, C.; Bucher, J. P. *Angew.Chem., Int. Ed.* **2007**, *46*, 2659.
(27) Du, P.; Scheineder, J.; Jarosz, P.; Zhang, J.; Brennessel, W. W.; Eisenberg, R. *J. Phys. Chem. B.* **2007**, *111*, 6887; and references therein.
(28) Shikhova, E.; Danilov, E. O.; Kinayyigit, S.; Pomestchenko, I. E.; Tregubov, A. D.; Camerel, F.; Retailleau, P.; Ziessel, R.; Castellano, F. N. *Inorg. Chem.* **2007**, *46*, 3038; and references therein.
(29) Kim, K. Y.; Liu, S.; Köse, M. E.; Schanze, K. S. *Inorg. Chem.* **2006**, *45*, 2509.
(30) Adams, C. J.; Fey, N.; Weinstein, J. A. *Inorg. Chem.* **2006**, *45*, 6105.
(31) Han, X.; Wu, L. Z.; Si, G.; Pan, J.; Yang, Q. Z.; Zhang, L. P.; Tung, C. H. *Chem.—Eur. J.* **2007**, *13*, 1231.
(32) Long, N. J.; Wong, C. K.; White, A. H. *Organometallics* **2006**, *25*, 2525.
(33) Silverman, E. E.; Cardolaccia, T.; Zhao, X.; Kim, K. Y.; Haskins-Glusac, K.; Schanze, K. S. *Coord. Chem. Rev.* **2005**, *249*, 1491.
(34) Wong, C. Y.; Che, C. M.; Chan, M. C.; Han, J.; Leung, K. H.; Phillips, D. L.; Wong, K. Y.; Zhu, N. *J. Am. Chem. Soc.* **2005**, *127*, 13997.
(35) Saha, K.; Qaium, M. A.; Debnath, D.; Younus, M.; Chawdhury, N.; Sultana, N.; Kociok Köhn, G.; Ooi, L. L.; Raithby, P. R.; Kijima, M. *Dalton Trans.* **2005**, 2760; and references therein.
(36) Lu, W.; Mi, B. X.; Chan, M. C. W.; Hui, Z.; Che, C. M.; Zhu, N.; Lee, S. T. *J. Am. Chem. Soc.* **2004**, *126*, 4958; and references therein.
(37) Fernández, S.; Forniés, J.; Gil, B.; Gómez, J.; Lalinde, E. *Dalton Trans.* **2003**, 822.
(38) Benito, J.; Berenguer, J. R.; Forniés, J.; Gil, B.; Gómez, J.; Lalinde, E. *Dalton Trans.* **2003**, 4331.
(39) Gil, B.; Forniés, J.; Gómez, J.; Lalinde, E.; Martín, A.; Moreno, M. T. *Inorg. Chem.* **2006**, *45*, 7788.
(40) Forniés, J.; Fuertes, S.; Martín, A.; Sicilia, V.; Lalinde, E.; Moreno, M. T. *Chem.—Eur. J.* **2006**, *12*, 8253.
(41) Fernández, J.; Forniés, J.; Gil, B.; Gómez, J.; Lalinde, E.; Moreno, M. T. *Organometallics* **2006**, *25*, 2274.
(42) Ara, I.; Berenguer, J. R.; Eguizábal, E.; Forniés, J.; Gómez, J.; Lalinde, E. *J. Organomet. Chem.* **2003**, *670*, 221.
(43) Berenguer, J. R.; Forniés, J.; Gómez, J.; Lalinde, E.; Moreno, M. T. *Organometallics* **2001**, *20*, 4847.
(44) Forniés, J.; Gómez, J.; Lalinde, E.; Moreno, M. T. *Inorg. Chem.* **2001**, *40*, 5415.
(45) Charmant, J. P. H.; Falvello, L. R.; Forniés, J.; Gómez, J.; Lalinde, E.; Moreno, M. T.; Orpen, A. G.; Rueda, A. *Chem. Commun.* **1999**, 2045; and references therein.
(46) Yin, G.-Q.; Wei, Q.-H.; Zhang, L. Y.; Chen, Z. N. *Organometallics* **2006**, *25*, 580.
(47) Chui, S. S. Y.; Ng, M. F. Y.; Che, C. M. *Chem.—Eur. J.* **2005**, *11*, 1739.
(48) Yip, S. K.; Cheng, E. C. C.; Yuan, L. H.; Zhu, N.; Yam, V. W. W. *Angew. Chem., Int. Ed.* **2004**, *43*, 4954.
(49) Wei, Q. H.; Yin, G. Q.; Zhang, L. Y.; Chen, Z. N. *Inorg. Chem.* **2006**, *45*, 10371; and references therein.
(50) Wei, Q. H.; Zhang, L. Y.; Yin, G. Q.; Shi, L.-X.; Chen, Z. N. *J. Am. Chem. Soc.* **2004**, *126*, 9940.
(51) Yam, V. W. W.; Hui, C. K.; Yu, S. Y.; Zu, N. *Inorg. Chem.* **2004**, *43*, 812; and references therein.
(52) Yam, V. W. W.; Chong, S. H. F.; Wong, K. M. C.; Cheung, K. K. *Chem.Commun.* **1999**, 1013.
(53) Wong, K. M. C.; Hui, C. K.; Yu, K. L.; Yam, V. W. W. *Coord. Chem. Rev.* **2002**, *229*, 123.
(54) Pyykkö, P. *Chem. Rev.* **1997**, *97*, 597.
(55) Pyykkö, P. *Angew. Chem., Int. Ed.* **2004**, *43*, 4412.
(56) Gade, L. H. *Angew. Chem., Int. Ed.* **2001**, *40*, 3573.
(57) Carvajal, M. A.; Álvarez, S.; Novoa, J. J. *Chem.—Eur. J.* **2004**, *10*, 2117.
(58) Sakai, K.; Ishigami, E.; Konno, Y.; Kajiwara, T.; Ito, T. *J. Am. Chem. Soc.* **2002**, *124*, 12088.
(59) Forward, J. M.; Fackler, J. P., Jr.; Assefa, Z. In *Optoelectronic Properties of Inorganic Compounds*; Roundhill, D. M., Fackler, J. P., Jr., Eds.; Plenum Press: New York, 1999, pp 195−239
(60) Elbjeirami, O.; Omary, M. A. *J. Am. Chem. Soc.* **2007**, *129*, 11384; and references therein.
(61) Fernández, E.; Laguna, A.; López de Luzuriaga, J. M. *Dalton Trans.* **2007**, 1969; and references therein.
(62) Che, C. M.; Lai, S. W. *Coord. Chem. Rev.* **2005**, *249*, 1296.
(63) Esswein, A. J.; Dempsey, J. L.; Nocera, D. G. *Inorg. Chem.* **2007**, *46*, 2362.
(64) Rasika, H. V.; Gamage, C. S. P.; Keltner, J.; Diyabalanage, H. V. K.; Omari, I.; Eyobo, Y.; Dias, N. R.; Roehr, N.; McKinney, L.; Poth, T. *Inorg. Chem.* **2007**, *46*, 2979.
(65) Lu, W.; Roy, V. A. L.; Che, C. M. *Chem.Commun.* **2006**, 3972; and references therein.
(66) Yang, C.; Messerschmidt, M.; Coppens, P.; Omary, M. A. *Inorg. Chem.* **2006**, *45*, 6592.
(67) White Morris, R. L.; Olmstead, M. M.; Attar, S.; Balch, A. L. *Inorg. Chem.* **2005**, *44*, 5021.
(68) Falvello, L. R.; Forniés, J.; Lalinde, E.; Menjón, B.; Garcia Monforte, M. A.; Moreno, M. T.; Tomás, M. *Chem.Commun.* **2007**, 3838.
(69) Bartolomé, C.; Carrasco-Rando, M.; Coco, S.; Cardovilla, C.; Espinet, P.; Martín-Álvarez, J. M. *Organometallics* **2006**, *25*, 2700.
(70) Coker, N. L.; Bauer, J. A. K.; Eder, R. C. *J. Am. Chem. Soc.* **2004**, *126*, 12.
(71) Stender, M.; White Morris, R. L.; Olmstead, M. M.; Balch, A. L. *Inorg. Chem.* **2003**, *42*, 4504.
(72) Xia, B. H.; Zhang, H. X.; Che, C. M.; Leung, K. H.; Phillips, D. L.; Zhu, N.; Zhou, Z. Y. *J. Am. Chem. Soc.* **2003**, *125*, 10362.
(73) Lee, Y. A.; McGarrah, J. E.; Lachicotte, R. J.; Eisenberg, R. *J. Am. Chem. Soc.* **2002**, *124*, 10662.
(74) Cariati, E.; Bu, X.; Ford, P. C. *Chem. Mater.* **2000**, *12*, 3385; and references therein.
(75) Díez, A.; Forniés, J.; Gómez, J.; Lalinde, E.; Martín, A.; Moreno, M. T.; Sánchez, S. *Dalton Trans.* **2007**, 3653.
(76) Maliarik, M.; Nagle, J. K.; Ilyukhin, A.; Murashova, E.; Mink, J.; Skripkin, M.; Glaser, J.; Kovacs, M.; Horváth, A. *Inorg. Chem.* **2007**, *46*, 4642.
(77) Chen, W.; Liu, F.; Xu, D. X.; Matsumoto, K.; Kishi, S.; Kato, M. *Inorg. Chem.* **2006**, *45*, 5552; and references therein.
(78) Falvello, L. R.; Forniés, J.; Garde, R.; García, A.; Lalinde, E.; Moreno, M. T.; Steiner, A.; Tomás, M.; Usón, I. *Inorg. Chem.* **2006**, *45*, 2543.
(79) Catalano, V. J.; Bennett, B. L.; Malwitz, M. A.; Yson, R. L.; Kar, H. M.; Muratidis, S.; Horner, S. J. *Comments Inorg. Chem.* **2003**, *24*, 24.
(80) Fernández, E.; Laguna, A.; López de Luzuriaga, J. M. *Coord. Chem. Rev.* **2005**, *249*, 1423.
(81) Wu, G.; Wang, D. *J. Cluster Sci.* **2007**, *18*, 408.
(82) Stork, J. R.; Olmstead, M. M.; Fettinger, J. C.; Balch, A. L. *Inorg. Chem.* **2006**, *45*, 849.
(83) Fernández, E. J.; Laguna, A.; López de Luzuriaga, J. M.; Montiel, M.; Olmos, M. E.; Pérez, J. *Organometallics* **2005**, *24*, 1631.
(84) Catalano, V. J.; Malwitz, M. A. *J. Am. Chem. Soc.* **2004**, *126*, 6560.
(85) Srisook, N.; Rizzolo, J.; Shankle, G. E.; Patterson, H. H. *Inorg. Chim. Acta* **2000**, *300−302*, 314.
(86) Catalano, V. J.; Bennett, B. L.; Yson, R. L.; Noll, B. C. *J. Am. Chem. Soc.* **2000**, *122*, 10056.
(87) Song, H. B.; Zhang, Z. Z.; Hui, H.; Che, C. M.; Mak, M. C. W. *Inorg. Chem.* **2002**, *41*, 3146.
(88) Catalano, V. J.; Bennett, B. L.; Kar, H. M. *J. Am. Chem. Soc.* **1999**, *121*, 10235.

bonds, only a handful of polymetallic d^{10}-Pb^{II}[79,93–95] and d^8-Pb^{II}[96–104] complexes have been reported, and little is known about their luminescence properties.[93–95,98–101]

Several years ago, Balch and co-workers noted the difficulty in obtaining bonding between Pt^{II} and Pb^{II} centers.[96] Thus, in contrast to the easy formation of Pt−Tl^{I} bonds which leads to $[PtTl_2(CN)_4]$,[105] the related system $Pb(NO_3)_2$-$K_2Pt(CN)_4$ gave the salt $K_2Pb[Pt(CN)_4]_2\cdot 6H_2O$ formed by zigzag Pt···Pt bonding columns of $[Pt(CN)_4]^{2-}$ ions with the Pb^{2+} and K^+ ions set off to the side of the columns.[96] By using $[Pt(CN)_2(\text{crown-}P_2)]$ (crown-P_2 = 1,10-bis((diphenylphosphino)-methyl)-1,10-diaza-4,7,13,16-tetraoxaoctadecane) as the building block, two related $[Tl(\text{crown-}P_2)Pt(CN)_2]^{+}$[92,96] and $[(CH_3CO_2)Pb(\text{crown-}P_2)Pt(CN)_2]^{+}$ bimetallic derivatives were formed. Despite the smaller size of the ion Pb^{II} in relation to Tl^{I},[106] the Pt^{II}−Tl^{I} bond (2.911(2), 2.958(2) Å) was found to be 0.40−0.35 Å shorter than the Pt^{II}−Pb^{II} (3.313(2) Å),[92,96] reflecting again the lesser ability of the $6s^2$ orbital of Pb to interact or overlap with orbitals on platinum. However, our group has successfully isolated the first two isoelectronic linear-chain trinuclear anionic $(NBu_4)_2[\{Pt(C_6F_5)_4\}_2Pb]$[97] and $(NBu_4)_3[\{Pt(C_6F_5)_4\}_2Tl]$[78] derivatives by reaction of $(NBu_4)_2[Pt(C_6F_5)_4]$ with $Pb(NO_3)_2$ and $Tl(NO_3)$, respectively. In contrast to previous observations, it is remarkable that the Pt^{II}−Pb^{II} bond distances (2.769(2) and 2.793(2) Å)[97] are clearly shorter than the Pt^{II}−Tl^{I} bonds (2.9777(4); 3.0434(4) Å),[78] a feature that cannot be attributed to the strength of the additional and close *o*-F···M contacts, which are only slightly shorter in the platinum lead derivative (2.761(2)−2.995(3) Å in $[Pt_2Pb]^{2-}$ versus 2.883(5)−2.988(6) Å in $[Pt_2Tl]^{3-}$). Stimulated by these observations and following our recent interest in heteropolynuclear platinum alkynyl based systems with d^{10} (Cu^{I}, Ag^{I}, Au^{I}, Cd^{II})[39–44,107–109] and Tl^{I}[43,110–112] heterometals of remarkable structural diversity and exhibiting rich luminescent properties, we have initiated an investigation aimed at the synthesis and study of the optical properties of related platinum−lead complexes. Encouraged by our success with pentafluorophenylplatinate precursors,[97–99] we set out to see whether related anionic Pt^{II} complexes, in which the C_6F_5 rings are replaced by alkynyl and/or chromophore groups such as benzoquinolate, might have a similar affinity toward Pb^{II} and how the variation in the electronic nature of the platinate fragment might affect the Pt−Pb interaction. As far as the $Pb^{II}\cdots\pi$ (alkyne or alkynide) interaction is concerned, to the best of our knowledge, it has not previously been reported. 1-Alkynyllead(IV) compounds $R'_{4-n}Pb(C{\equiv}C{-}R)_n$ are known,[113] and the zwitterionic complex $[{}^{i}Pr_2B^{-}$-$(C({}^{i}Pr){=}CMe)(\mu\text{-}C{\equiv}CMe)Pb^{+}Me_2]$, obtained from the 1,1-organoboration reaction between $^{i}Pr_3B$ and $Me_2Pb(C{\equiv}CMe)_2$, is the only example characterized by X-ray analysis in which an alkynyl group was found to coordinate a "free" triorganolead cation.[114] This study may thus allow us to observe the possible competition between the basic platinum center and the alkynyl fragment to bond the Pb^{II}.

In the current work we report the synthesis and structural characterization of novel angular $[Pt]_2Pb$ systems and provide a detailed study of the luminescence properties of these complexes together with those of the previously reported linear derivative $(NBu_4)_2[\{Pt(C_6F_5)_4\}_2Pb]$[97] **5**.

Experimental Section

Materials and Methods. The reactions were performed under an Ar atmosphere, and the solvents were purified by standard methods (CH_2Cl_2 and *n*-hexane were distilled over CaH_2 and acetone was treated and then distilled over $KMnO_4$. However, the MeTHF was employed as received). Elemental analyses, conductivities, and IR, mass, and ^1H NMR spectroscopies were performed as described elsewhere.[115] The low stability of complexes **1** and **2** and the low solubility of **3** and **4** precludes its characterization by $^{13}C\{^1H\}$ and ^{195}Pt NMR spectroscopy. UV−vis spectra were recorded on a Hewlet Packard 8453 spectrometer. Diffuse reflectance UV−vis (DRUV) spectra of pressed powder were recorded on a Unicam UV-4 spectrophotometer with an integrating sphere accessory of the Spectralon RSA-UC-40 Labsphere type. Excitation and emission spectra were obtained on a Jobin-Yvon Horiba Fluorolog 3−11 Tau-3 spectrofluorimeter. The lifetime measurements were performed operating in the phase-modulation mode

(89) Casado, M. A.; Pérez-Torrente, J. J.; López, J. A.; Ciriano, M. A.; Lahoz, F. J.; Oro, L. A. *Inorg. Chem.* **1999**, *382*, 482.
(90) Usón, R.; Forniés, J.; Tomás, M.; Garde, R. *Inorg. Chem.* **1997**, *36*, 1383.
(91) Balch, A. L.; Nagle, J. K.; Olmstead, M. M.; Reddy, P. E., Jr *J. Am. Chem. Soc.* **1987**, *109*, 4123.
(92) Balch, A. L.; Rowley, S. P. *J. Am. Chem. Soc.* **1990**, *112*, 6139.
(93) Catalano, V. J.; Bennett, B. L.; Noll, B. C. *Chem.Commun.* **2000**, 1413.
(94) Wang, S.; Garzón, G.; King, C.; Wang, J. C.; Fackler, J. P., Jr *Inorg. Chem.* **1989**, *28*, 4623.
(95) Patterson, H. H.; Bourassa, J.; Shankle, G. *Inorg. Chim. Acta* **1994**, *226*, 345.
(96) Balch, A. L.; Fung, E. Y.; Nagle, J. K.; Olmstead, M. M.; Rowley, S. P. *Inorg. Chem.* **1993**, *32*, 3295.
(97) Usón, R.; Forniés, J.; Falvello, L. R.; Usón, M. A.; Usón, I. *Inorg. Chem.* **1992**, *31*, 3697.
(98) Ara, I.; Falvello, L. R.; Forníes, J.; Gómez-Cordón, J.; Lalinde, E.; Merino, R. I.; Usón, I. *J. Organomet. Chem.* **2002**, *663*, 284; and references therein.
(99) Casas, J. M.; Forniés, J.; Martín, A.; Orera, V. M.; Orpen, A. G.; Rueda, A. *Inorg. Chem.* **1995**, *34*, 6514.
(100) Balch, A. L.; Catalano, V. J.; Chatfield, M. A.; Nagle, J. K.; Olmstead, M. M.; Reedy, P. E., Jr *J. Am. Chem. Soc.* **1991**, *113*, 1252.
(101) Balch, A. L.; Neve, F.; Olmstead, M. M. *Inorg. Chem.* **1991**, *30*, 3395.
(102) Albano, V. G.; Castellari, C.; Monari, M.; DeFelice, V.; Ferrara, M. L.; Ruffo, F. *Organometallics* **1995**, *14*, 4213.
(103) Crociani, B.; Nicolini, M.; Clemente, D. A.; Bandoli, G. *J. Organomet. Chem.* **1973**, *49*, 249.
(104) Zhou, M.; Xu, Y.; Lam, C. F.; Koh, L. L.; Mok, K. F.; Leung, P. H.; Hor, T. S. A. *Inorg. Chem.* **1993**, *32*, 4660.
(105) Nagle, J. K.; Balch, A. L.; Olmstead, M. M. *J. Am. Chem. Soc.* **1988**, *110*, 319.
(106) Shannon, R. D. *Acta Crystallogr.* **1976**, *A32*, 751.
(107) Charmant, J. P. H.; Forniés, J.; Gómez, J.; Lalinde, E.; Merino, R.; Moreno, M. T.; Orpen, A. G. *Organometallics* **1999**, *18*, 3353.
(108) Ara, I.; Forniés, J.; Gómez, J.; Lalinde, E.; Moreno, M. T. *Organometallics* **2000**, *19*, 3137.
(109) Forniés, J.; Ibáñez, S.; Martín, A.; Gil, B.; Lalinde, E.; Moreno, M. T. *Organometallics* **2004**, *23*, 3963.
(110) Ara, I.; Berenguer, J. R.; Forniés, J.; Gómez, J.; Lalinde, E.; Martín, A.; Merino, R. *Inorg. Chem.* **1997**, *36*, 6461.
(111) Charmant, J. P. H.; Forniés, J.; Gómez, J.; Lalinde, E.; Merino, R. I.; Moreno, M. T.; Orpen, A. G. *Organometallics* **2003**, *22*, 652.
(112) Berenguer, J. R.; Forniés, J.; Gil, B.; Lalinde, E. *Chem.—Eur. J.* **2006**, *12*, 785.
(113) Wrackmeyer, B. *Coord. Chem. Rev.* **1995**, *145*, 125.
(114) Wrackmeyer, B.; Horchler, K.; Boese, R. *Angew.Chem., Int. Ed. Engl.* **1989**, *28*, 1500.
(115) Berenguer, J. R.; Lalinde, E.; Torroba, J. *Inorg. Chem.* **2007**, *46*, 9919.

(phase shift and modulation in the frequency range of 0.1−10 MHz) or in the phosphorimeter mode (with a F1−1029 lifetime emission PMT assembly, using a 450 W Xe lamp). Quantum yields in solid state were measured upon excitation at 450 nm using a F-3018 Integrating Sphere mounted on a Fluorolog 3−11 Tau-3 spectrofluorimeter. Data were fitted using the Jobin-Yvon software package. $(NBu_4)_2[Pt(C{\equiv}CTol)_4]$,[38] $(NBu_4)[Pt(bzq)(C{\equiv}CR)_2]$ (R = Ph, $C_6H_4-CF_3$-4)[37] and $(NBu_4)_2[\{Pt(C_6F_5)_4\}_2Pb]$[97] **5** were prepared as reported. $(NBu_4)[Pt(bzq)(C{\equiv}CPh)_2]$ ^{1}H NMR (δ, $CDCl_3$, 400.13 MHz): 10.04 (d, J_{H-H} = 4.9 Hz, $^3J_{Pt-H}$ = 23.6 Hz, H^2, bzq), 8.56 (d, J_{H-H} = 5.6 Hz, $^3J_{Pt-H}$ = 40.0 Hz, H^9, bzq), 8.20 (d, J_{H-H} = 7.6 Hz, H^4, bzq), 7.70 (d, J_{H-H} = 8.7 Hz, H^5, bzq), 7.50 (m, H^8 + Ph), 7.45 (m, J_{H-H} = 8.6 Hz, H^6, bzq), 7.40 (Ph), 7.37 (m, H^3, bzq), 7.18 (m, Ph), 7.07 (m, Ph), 3.18 (NCH_2, NBu_4), 1.21 (m, CH_2), 1.01 (m, CH_2), 0.6 (t, CH_3, NBu_4).

Preparation of $(NBu_4)_2[\{Pt(C{\equiv}CTol)_4\}_2Pb(OH_2)_2]$ (1). $Pb(ClO_4)_2{\cdot}3H_2O$ (0.040 g, 0.088 mmol) was added into a colorless solution of $(NBu_4)_2[Pt(C{\equiv}CTol)_4]$ (0.200 g, 0.175 mmol) in acetone (30 mL). The color of the reaction solution immediately changed to deep yellow. After stirring for 30 min, the solution was concentrated to a small volume (∼5 mL) and cooled (−30 °C) overnight. The deep yellow solid obtained **1** was filtered and washed with cold acetone. When the solid is air-dried in the filter its color changes to pale yellow (0.073 g, 41%). Anal. Calcd for $C_{104}H_{132}N_2O_2PbPt_2$: C, 61.25; H, 6.52; N, 1.37. Found: C, 61.50; H, 6.25; N 1.42. Λ_M: 142.6 (acetone), 122.5 ($MeNO_2$) $\Omega^{-1}{\cdot}cm^2{\cdot}mol^{-1}$. MS (Maldi+): *m/z* 2246.3 $[M + Pb]^+$, 58%; 2211 $[M - 2H_2O + Pb]^+$, 20%. IR (cm^{-1}): ν(C≡C) 2097 (s), ν(OH, H_2O) 3375 (br). ^{1}H NMR (δ, 300.13 MHz, $CDCl_3$): 7.17 (d, J = 7.3 Hz, 16H, C_6H_4, Tol), 6.88 (d, J = 7.3 Hz, 16H, C_6H_4, Tol), 3.56 (m, 16H, NCH_2, NBu_4), 2.24 (s, 24H, CH_3, Tol), 1.62 (m, 16H, CH_2, NBu_4), 1.47 (m, 16H, CH_2, NBu_4), 0.85 (t, 24H, CH_3, NBu_4).

Preparation of $[\{Pt(bzq)(C{\equiv}CPh)_2\}_2Pb]$ (2). $Pb(ClO_4)_2{\cdot}3H_2O$ (0.056 g, 0.123 mmol) was added to a yellow solution of $(NBu_4)[Pt(bzq)(C{\equiv}CPh)_2]$ (0.200 g, 0.246 mmol) in 10 mL of acetone. The color of the solution changed to orange and an orange precipitate appeared, which was filtered and washed with cold acetone (0.136 g, 82%). Anal. Calcd for $C_{58}H_{36}N_2PbPt_2$: C, 51.29; H, 2.67; N, 2.06. Found: C, 51.43; H, 2.79; N 2.13. Λ_M: 26.8 (N,N-dimethylformamide), 2.43(CH_2Cl_2) $\Omega^{-1}{\cdot}cm^2{\cdot}mol^{-1}$. MS (ES+): *m/z* 1359 $[M + H]^+$, 100%. IR (cm^{-1}): ν(C≡C) 2080 (m), 2017 (sh). ^{1}H NMR (δ, 300.13 MHz, $CDCl_3$): 8.94 (d, J_{H-H} = 5.0 Hz, $^3J_{Pt-H}$ = 30 Hz, 2H, H^2, bzq), 8.39 (d, J_{H-H} = 6.5 Hz, $^3J_{Pt-H}$ = 42.5 Hz, 2H, H^9, bzq), 7.54, 7.45, 7.26, 7.19 (CH, 28H, bzq, Ph), 7.06 (d, J = 7.8 Hz, 2H, bzq), 6.39 (dd, J_{H-H} = 7.4, 5.5 Hz, 2H, H^3, bzq).

Reaction of $(NBu_4)[Pt(bzq)(C{\equiv}CC_6H_4-CF_3\text{-}4)_2]$ with $Pb(ClO_4)_2{\cdot}3H_2O$. Synthesis of $[\{Pt(bzq)(C{\equiv}CC_6H_4-CF_3\text{-}4)_2\}_2Pb]$ (3) (method 1) and $(NBu_4)[\{Pt(bzq)(C{\equiv}CC_6H_4-CF_3\text{-}4)_2\}_2Pb(O_2ClO_2)]$ (4). A yellow solution of $(NBu_4)[Pt(bzq)(C{\equiv}CC_6H_4-CF_3\text{-}4)_2]$ (0.100 g, 0.105 mmol) in acetone (10 mL) was treated with $Pb(ClO_4)_2{\cdot}3H_2O$ (0.024 g, 0.052 mmol) and the mixture stirred for 5 min. The solvent was removed, and CH_2Cl_2 (∼10 mL) was added to the resulting orange residue, affording **3** as an orange solid (0.023 g, 8.5%). By addition of *n*-hexane to the filtrate and keeping the mixture in the freezer overnight, the adduct $(NBu_4)[\{Pt(bzq)(C{\equiv}CC_6H_4-CF_3\text{-}4)_2\}_2Pb(O_2ClO_2)]$ **4** precipitated as a yellow microcrystalline solid. When the solid is dried, its color changes to orange (0.040 g, 39%).

$[\{Pt(bzq)(C{\equiv}CC_6H_4-CF_3\text{-}4)_2\}_2Pb]$ (3) (method 2). A solution of $(NBu_4)[Pt(bzq)(C{\equiv}CC_6H_4-CF_3\text{-}4)_2]$ (0.200 g, 0.210 mmol) in acetone was treated with excess of $Pb(ClO_4)_2{\cdot}3H_2O$ (0.096 g, 0.210 mmol). After stirring the mixture for 5 min, the solvent was removed and CH_2Cl_2 (∼10 mL) was added to the residue. The resulting orange solid was filtered, washed repeatedly with H_2O, and air-dried (0.135 g, 79%).

Data for 3. Anal. Calcd for $C_{62}H_{32}F_{12}N_2Pt_2Pb$: C, 45.68; H, 1.98; N, 1.72. Found: C, 45.37; H, 1.75; N, 1.83. Λ_M: 153 $\Omega^{-1}{\cdot}cm^2$ mol^{-1} (acetone). MS (Maldi-): *m/z* 1461.3 $[M-C{\equiv}CC_6H_4-CF_3]^+$, 5%. IR ($cm^{-1}$): ν(C≡C) 2099 (s); 2072 (m). ^{1}H NMR (δ, 300.13 MHz, CD_3COCD_3): 9.06 (d, J_{H-H} = 4.0 Hz, $^3J_{Pt-H}$ ≈ 31.3 Hz, 2H, H^2, bzq), 8.33 (m br, $^3J_{Pt-H}$ = 46.0 Hz, 2H, H^9, bzq), 7.82 (d, J_{H-H} = 7.5 Hz, 2H, H^4, bzq), 7.66 (d, 4H), 7.55 (m, 18H), 7.30 (d, J_{H-H} = 8.4 Hz, 2H) (C_6H_4/bzq), 6.68 (t, J_{H-H} = 5.7 Hz, 2H, H^8, bzq). ^{19}F NMR (δ, 282.4 MHz, CD_3COCD_3): −144.87 (s br, CF_3).

Data for 4. Anal. Calcd for $C_{78}ClF_{12}H_{68}N_3O_4PbPt_2$: C, 47.50; H, 3.48; N, 2.13. Found: C, 47.43; H, 3.50; N, 2.25. Λ_M: 100.3 $\Omega^{-1}{\cdot}cm^2{\cdot}mol^{-1}$ (acetone). MS (ES-): *m/z* 711 $[Pt(bzq)(C{\equiv}CC_6H_4-CF_3-4)_2]^-$, 100%. IR ($cm^{-1}$): ν(C≡C) 2092 (m), 2080 (m); $\nu(O_2ClO_2)$ 622(s), 598(s) cm^{-1}, bands due to $O_2ClO_2^-$ around 1100 cm^{-1} cannot be unambiguously assigned because of overlapping with $C_6H_4-CF_3$-4 bands. ^{1}H NMR (δ, 300.13 MHz, CD_3COCD_3): 9.07 (d, J_{H-H} = 4.6 Hz, $^3J_{Pt-H}$ ≈ 30.9, 2H, H^2, bzq), 8.33 (dd, J_{H-H} = 4.5, 3.4 Hz, $^3J_{Pt-H}$ = 41.8 Hz, 2H, H^9, bzq), 7.83 (d, J_{H-H} = 7.8 Hz, 2H, H^4, bzq), 7.67 (d, 4H), 7.53 (m, 18H), 7.30 (d, J_{H-H} = 8.7 Hz, 2H) (C_6H_4/bzq), 6.70 (dd, J_{H-H} = 8.3, 5.6 Hz, 2H, H^8, bzq), 3.42 (m, 8H, CH_2, NBu_4), 1.80 (m, 8H, CH_2, NBu_4), 1.42 (m, 8H, CH_2, NBu_4), 0.96 (t, 12H, CH_3, NBu_4). ^{19}F NMR (δ, 282.4 MHz, CD_3COCD_3): −144.88 (s br, CF_3).

X-ray Crystallography. Tables 1 and 2 report details of the structural analyses for all complexes. Yellow (**1**, **4**) or orange (**2**) crystals were obtained by slow diffusion of diethylether (**1**) or *n*-hexane (**2**, **4**) into dichloromethane (**1**, **2**, −30 °C) or dichloromethane/methanol (**4**, −30 °C) solutions of each compound. For complex **1** three and a half-molecules of dichloromethane and for complex **4** one molecule of methanol and three of water were found in the asymmetric unit. X-ray intensity data were collected with a NONIUS-κCCD area-detector diffractometer, using graphite-monochromated Mo Kα radiation. Images were processed using the DENZO and SCALEPACK suite of programs,[116] carrying out the absorption correction at this point for complexes **2** and **4**. For complex **1**, the absorption correction was performed using MULTISCAN.[117] The structure of **1** was solved by Direct Methods using SHELXS-97,[118] while those of **2** and **4** were solved by Patterson and Fourier methods using DIRDIF92.[119] The structures were refined by full-matrix least-squares on F^2 with SHELXL-97,[118] and all non-hydrogen atoms were assigned anisotropic displacement parameters. The hydrogen atoms were constrained to idealized geometries fixing isotropic displacement parameters 1.2 times the U_{iso} value of their attached carbon for the aromatic and CH_2 hydrogens and 1.5 times for the methyl groups.

For complex **1**, which crystallizes in the non-centrosymmetric space group *Cc*, the crystal chosen for this structural analysis was found to be a meroedric twin, as confirmed by the absolute structure parameter (0.494(5)). However, inspection of the symmetry (using

(116) Otwinowski, Z.; Minor, W. In *Methods in Enzymology*; Carter, C. V., Jr., Sweet, R. M., Eds.; Academic Press: New York, 1997; Vol. *276A*, p 307.
(117) Blessing, R. H. *Acta Crystallogr.* **1995**, *A51*, 33.
(118) Sheldrick, G. M. *SHELX-97, a program for the refinement of crystal structures*; University of Göttingen: Germany, 1997.
(119) Beursken, P. T.; Beursken, G.; Bosman, W. P.; de Gelder, R.; García-Granda, S.; Gould, R. O.; Smith, J. M. M.; Smykalla, C. *The DIRDIF92 program system*; Technical Report of the Crystallography Laboratory: University of Nijmegen: The Netherlands, 1992.

Table 1. Crystallographic Data for **1**·3.5CH_2Cl_2, **2**, and **4**·CH_3OH·3H_2O

	1·3.5CH_2Cl_2	**2**	**4**·CH_3OH·3H_2O
empirical formula	$C_{107.5}H_{135}Cl_7O_2N_2PbPt_2$	$C_{58}H_{36}N_2PbPt_2$	$C_{79}H_{72}ClF_{12}N_3O_8PbPt_2$
f_w	2332.70	1358.26	2052.22
T (K)	123(1)	128(1)	173(1)
cryst syst, space group	monoclinic, *Cc*	orthorhombic, *Pnaa*	monoclinic, *P*21/*n*
a (Å)	22.7743(3)	12.5149(2)	12.6490(2)
b (Å)	17.2298(3)	19.5368(3)	18.7170(3)
c (Å)	27.3240(4)	36.8169(7)	33.6700(6)
α (deg)	90	90	90
β (deg)	101.4820(10)	90	96.9160(10)
γ (deg)	90	90	90
volume (Å^3)	10507.3(3)	9001.8(3)	7913.4(2)
Z	4	8	4
D_{calcd} (Mg/m^3)	1.475	2.004	1.723
abs coeff (mm^{-1})	4.480	9.974	5.766
F(000)	4668	5088	3976
θ range for data collection (deg)	3.59 to 25.68	2.01 to 27.52	2.20 to 27.96
no. of data/restraints/params	19586/4/1119	9448/30/592	17742/0/961
GOF onF^2 [a]	1.023	1.026	1.036
final R indices [$I > 2\sigma(I)$][a]	R1 = 0.0374, wR2 = 0.0883	R1 = 0.0582, wR2 = 0.0877	R1 = 0.0697, wR2 = 0.1001
R indices (all data)[a]	R1 = 0.0457, wR2 = 0.0926	R1 = 0.1140, wR2 = 0.1020	R1 = 0.1411, wR2 = 0.1187
largest diff peak and hole (e·Å^{-3})	1.763 and −1.688	1.456 and −1.275	1.637 and −1.325

[a] $R1 = \sum||F_o| - |F_c||/\sum|F_o|$; $wR2 = [\sum w(F_o^2 - F_c^2)^2/\sum wF_o^2]^{1/2}$; goodness of fit = $\{\sum[w(F_o^2 - F_c^2)^2]/(N_{obs} - N_{param})\}^{1/2}$; $w = [\sigma^2(F_o) + (g_1P)^2 + g_2P]^{-1}$; $P = [\max(F_o^2; 0 + 2F_c^2]/3$.

Table 2. Selected Bond Lengths (Å) and Angles (deg) for **1**·3.5CH_2Cl_2,[a] **2**, and **4**·CH_3OH·3H_2O

	$(NBu_4)_2[\{Pt(C\equiv CTol)_4\}_2Pb(OH_2)_2]$·3.5$CH_2Cl_2$ (1·3.5CH_2Cl_2)		
Pt(1)−Pb(1b)	2.9109(5)	$C^\alpha-C^\beta$	1.171(11)−1.260(12)
Pt(2)−Pb(1b)	2.8908(5)	Pb(1b)−O(1b)	2.469(8)
Pt−C^α	1.967(9)−2.032(9)	Pb(1b)−O(2b)	2.439(10)
Pt(1)−Pb(1b)−Pt(2)	149.95(2)	O(2b)−Pb(1b)−Pt(2)	83.60(18)
O(1b)−Pb(1b)−O(2b)	92.0(3)	$C^\alpha-Pt-C^\alpha$	88.1(4)−92.0(4)
O(1b)−Pb(1b)−Pt(1)	75.73(6)	Pt(1)−$C^\alpha-C^\beta$	174.2(8)−177.2(8)
O(1b)−Pb(1b)−Pt(2)	77.78(16)	Pt(2)−$C^\alpha-C^\beta$	173.5(8)−177.5(8)
O(2b)−Pb(1b)−Pt(1)	83.39(18)	$C^\alpha-C^\beta-C^\gamma$	174.1(10)−177.2(8)
	$[\{Pt(bzq)(C\equiv CPh)_2\}_2Pb]$ (2)		
Pt−C^α	1.973(11)−2.018(12)	$C^\alpha-C^\beta$	1.215(14)−1.233(12)
Pt−N(bzq)	2.058(8), 2.088(8)	Pt−C_{orth}	2.054(10), 2.061(9)
Pb(1)−Pt(1)	2.9759(5)	Pb(1)−C(2)	3.00(1)
Pb(1)−Pt(2)	2.9182(5)	Pb(1)−C(10)	3.063(9)
Pb(1)−C(1)	2.628(10)	Pb−C(31)	3.22(1)
Pb(1)−C(9)	2.682(9)	Pb−C(39)	3.07(1)
Pb(1)−C(30)	2.668(10)	Pt(1)−Pt(2)	3.5794(5)
Pb(1)−C(38)	2.619(9)		
Pt(1)−Pb(1)−Pt(2)	74.782(14)	Pt(2)−C(30)−C(31)	178.0(10)
C(1)−Pt(1)−C(9)	90.6(4)	C(1)−C(2)−C(3)	176.8(11)
C(38)−Pt(2)−C(30)	92.6(4)	C(9)−C(10)−C(11)	175.1(10)
Pt(1)−C(9)−C(10)	172.9(8)	C(38)−C(39)−C(40)	173.2(11)
Pt(1)−C(1)−C(2)	173.1(9)	C(30)−C(31)−C(32)	175.4(12)
Pt(2)−C(38)−C(39)	170.7(10)		
	$(NBu_4)[\{Pt(bzq)(C\equiv CC_6H_4\text{-}CF_3\text{-}4)_2\}_2Pb(O_2ClO_2)]$ CH_3OH·3H_2O (4·CH_3OH·3H_2O)		
Pt−C^α	1.962(10)−2.037(9)	$C^\alpha-C^\beta$	1.193(12)−1.217(12)
Pt−N(bzq)	2.058(10), 2.072(7)	Pt−C_{orth}	2.029(8), 2.050(9)
Pb(1)−Pt(1)	2.8715(5)	Pb(1)−C(11)	3.33(1)
Pb(1)−Pt(2)	3.3136(5)	Pb(1)−O(1)	2.880(8)
Pb(1)−C(1)	2.731(9)	Pb(1)−O(2)	3.013(8)
Pb(1)−C(10)	2.772(10)	Pb(1)−C(41)	2.659(10)
Pb(1)−C(2)	3.293(9)	Pb(1)−C(42)	2.94(1)
Pb(1)−C(32)	2.630(9)	Pt(1)−Pt(2)	3.8185(5)
Pb(1)−C(33)	2.94(1)		
Pt(1)−Pb(1)−Pt(2)	75.873(13)	C(10)−C(11)−C(12)	174.5(11)
C(1)−Pt(1)−C(10)	94.0(4)	Pt(2)−C(32)−C(33)	175.3(9)
C(32)−Pt(2)−C(41)	96.5(4)	Pt(2)−C(41)−C(42)	174.0(9)
Pt(1)−C(1)−C(2)	178.8(8)	C(32)−C(33)−C(34)	172.3(11)
Pt(1)−C(10)−C(11)	177.7(9)	C(41)−C(42)−C(43)	176.2(11)
C(1)−C(2)−C(3)	172.5(10)		

[a] These lengths and angles are comparable to those found for the minor components of the positional disorder in **1**·3.5CH_2Cl_2 (Pb(1a), O(1a), O(2a) 26%).

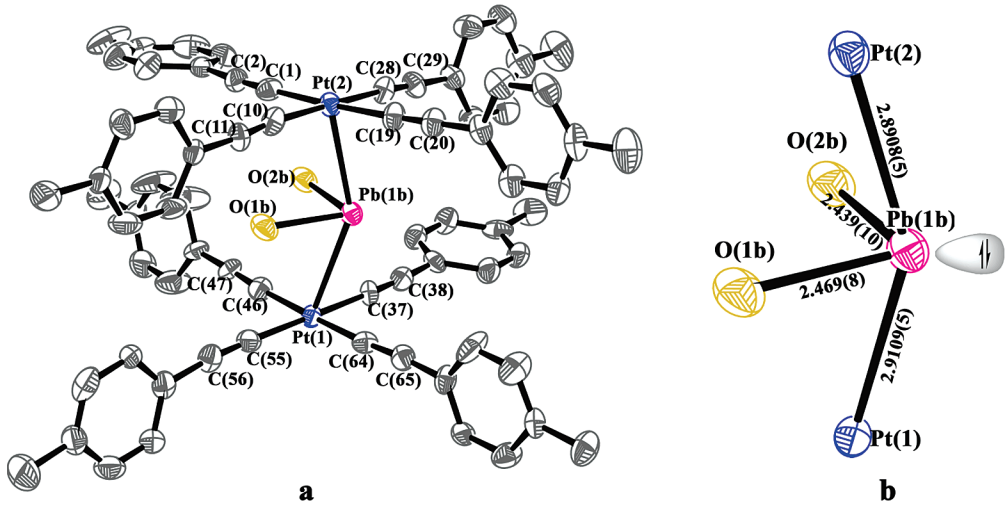

Figure 1. (a) Molecular structure of the major component in the positional disorder showed by the anion $[\{Pt(C{\equiv}CTol)_4\}_2Pb(OH_2)_2]^{2-}$ in **1** (major component). Ellipsoids are drawn at 50% probability level and hydrogen atoms omitted for clarity. (b) Hemidirected trigonal bipyramid coordination around the lead center, showing the presumed location for the lone pair.

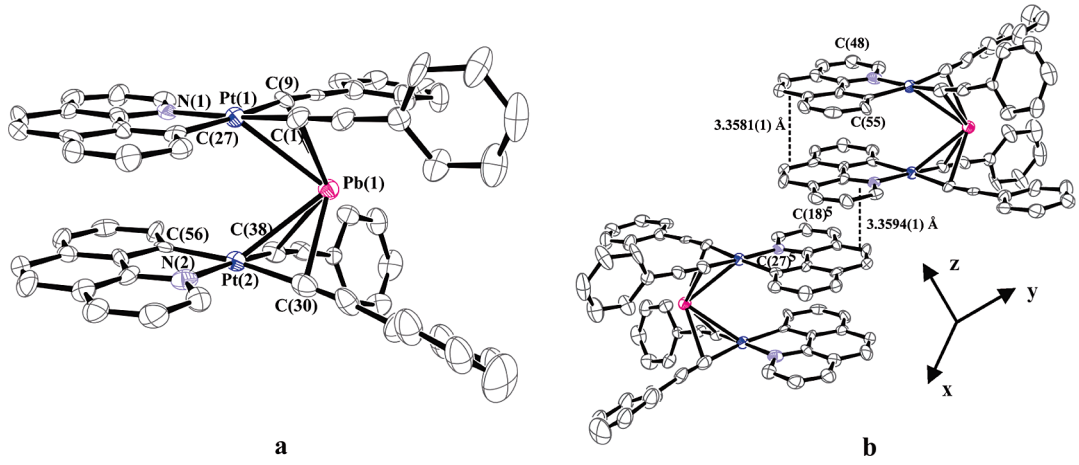

Figure 2. (a) ORTEP (Oak Ridge Thermal Ellipsoid Plot) view of $[\{Pt(bzq)(C{\equiv}CPh)_2\}_2Pb]$ **2** with the ellipsoids drawn at the 50% probability and the hydrogen atoms omitted for clarity. (b) Dimers generated by short $\pi\cdots\pi$ stacking interactions (~3.36Å).

Platon[120]) reveals the possibility of the existence of an inversion center. Thus, the structure has also been solved and refined in the centrosymmetric group *C*2/*c*, but with poorer results. Besides, for complex **1**, the Pb atom and the two water molecules binding to it present positional disorder, which has been refined over two positions with partial occupancy factors of 0.74 (Pb(1b), O(1b), O(2b))/0.26 (Pb(1a), O(1a), O(2a)). For this structure, one of the CH_2Cl_2 molecules also presents disorder, which has been adequately modeled. For complex **2**, two phenyl groups (C(3)−C(8) and C(32)−C(37)) present positional disorder, which was refined over two positions with partial occupancy factors of 0.5. In these two rings, as well as in the phenyl group C(11)−C(16), the carbon−carbon distances were constrained to a distance of 1.39(2) Å.

To establish the identities of the N and metalated C atoms of the 7,8-benzoquinoline ligand, the structures for **2** and **4**·CH_3OH·$3H_2O$ were refined in nine different ways (with the identities of the C and N of each ligand in one position, with the element types reversed, and with a 50/50 hybrid scattering factor at each of the affected atomic sites). Examination of the ΔMSDA values for bonds involving these atoms[120,121] revealed the following assignments: For complex **2** that is depicted in Figure 2a, the nitrogen atoms are in opposite positions for both of the bzq systems. For complex **4**, the position of the N and metalated C around Pt(1) are fixed (Figure 3), while the atoms around Pt(2) present a 50/50 hybrid scattering factor at each of the affected atomic sites. Thus, for **4**, both of the situations (with the nitrogen atoms in opposite positions, or one in front of the other) are crystallographically present. Finally, the three structures present some residual peaks greater than 1 e $Å^{-3}$ in the vicinity of the metal atoms or the crystallization solvent (for **1** and **4**) but with no chemical meaning.

Results and Discussion

Synthesis and Characterization. The synthesis of complexes **1**−**4** is summarized in Scheme 1. The reaction of $(NBu_4)_2[Pt(C{\equiv}CTol)_4]$ with $Pb(ClO_4)_2\cdot 3H_2O$ (0.5 equiv) in acetone yielded a yellow solution from which a deep yellow solid precipitated by partial elimination of solvent. When the solid is filtrated and air-dried the intensity of its initial color gradually decreases, leading to a pale yellow solid, which analyzes as $(NBu_4)_2[\{Pt(C{\equiv}CTol)_4\}_2Pb(OH_2)_2]$ **1** (45% yield). The observation of the characteristic $\nu(C{\equiv}C)$ absorption in its IR spectrum, slightly shifted to higher wavenumbers (2097 cm^{-1}) in relation to the precursor (2082

(120) Speck, A. L. *Acta Crystallogr.* **1990**, *A46*, C.
(121) Hirshfeld, F. L. *Acta Crystallogr., Sect. A* **1976**, *32*, 239.

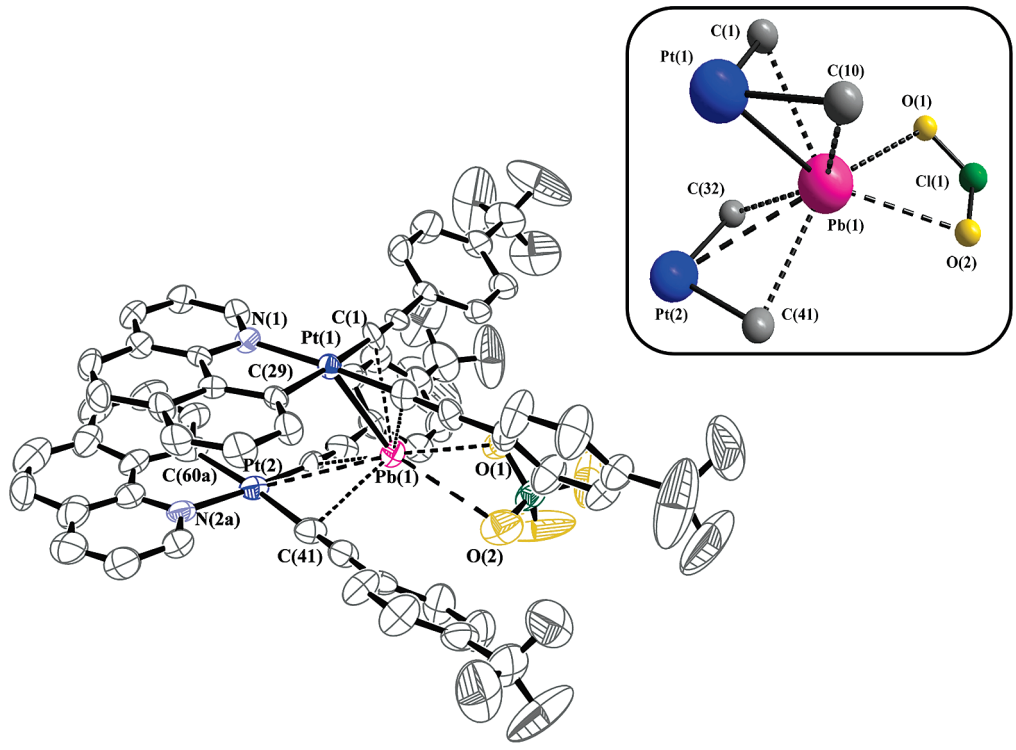

Figure 3. Molecular structure of the adduct anion $[\{Pt(bzq)(C{\equiv}CC_6H_4{-}CF_3\text{-}4)_2\}_2Pb(O_2ClO_2)]^-$ in **4**, with the coordination around the Pb^{II} in the inset. Ellipsoids are drawn at 50% probability level. Hydrogen atoms are omitted for clarity.

Scheme 1

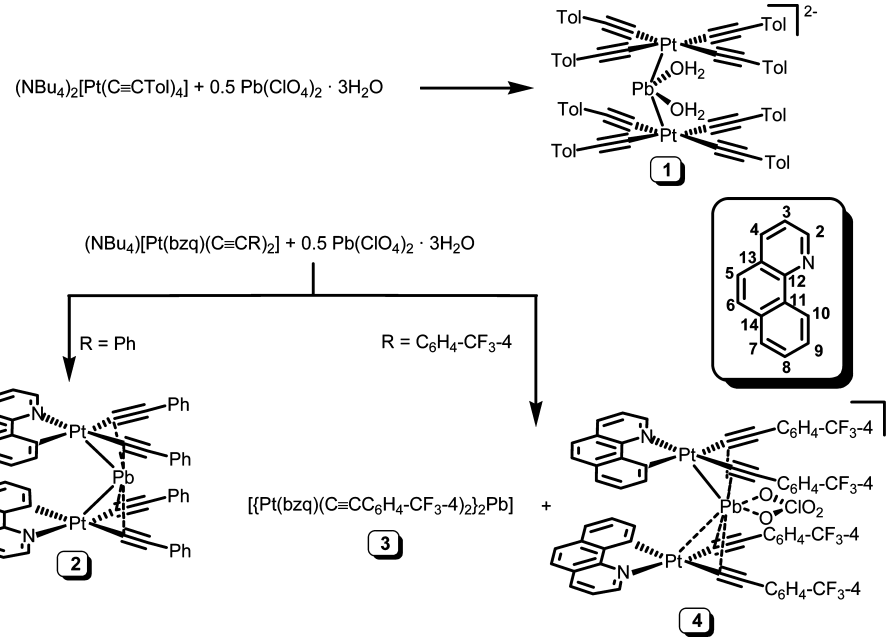

cm^{-1}), indicates that the interaction of the lead center with the alkynyl fragments is negligible. In fact, the small shift to higher frequencies points to the presence of Pt→Pb donor→acceptor bonds. We have previously observed that the formation of Pt→Tl bonding interactions somewhat reduces the π-back-donor component (Pt→π^*(C≡CR)) in the alkynyl platinate, increasing the strength of the ν(C≡C) vibration.[112] Additionally, the presence of a band at about 3375 cm^{-1} is in agreement with the presence of H_2O, which is further confirmed by X-ray crystallography. Conductivity measurements in acetone (142.6 $\Omega^{-1}\cdot cm^2\cdot mol^{-1}$) or nitromethane (122.5 $\Omega^{-1}\cdot cm^2\cdot mol^{-1}$) are in agreement with behavior as a 2:1 electrolyte.[122] Finally, the ^{1}H NMR spectrum of **1** indicates the presence of only one set of alkynyl fragments and the adequate integration with the signals of the NBu_4^+ cation. In addition, to examine the integrity of the trinuclear unit in solution, a small amount of the precursor $(NBu_4)_2[Pt(C{\equiv}CTol)_4]$ was added to a

(122) Geary, W. J. *Coord. Chem. Rev.* **1971**, *7*, 81.

solution of **1** in both CD_2Cl_2 and CD_3COCD_3. In both cases, the room temperature proton NMR spectrum exhibits, in the aromatic region, signals due to separated $[AB]_2$ systems: the starting material and complex **1**, thus indicating that dissociation of the $[Pt(C{\equiv}CTol)_4]^{2-}$ fragment does not occur or it is very slow on the NMR time scale. On standing, the solutions get darker, and signals due to **1** disappear in about 2 h suggesting a low stability of this complex in solution. We have examined the possibility to dehydrate complex **1** by heating a small solid amount (~20 mg) in a quartz tube using an oil bath. Unfortunately, it starts to darken at about 60−70 °C and after 5 min at ~90 °C it decomposes completely becoming black. To verify its composition, we performed a crystallographic study of crystals obtained by slow diffusion of diethylether into a solution of the solid **1** in CH_2Cl_2 at −30 °C. The crystal structure (Tables 1 and 2, Figure 1a,b) confirms the formation of a surprising diaqua diplatinum−lead anionic derivative, in which the Pb atom and the aqua ligands show positional disorder over two positions (0.24 **A**/0.76 **B** partial occupancy factors) with comparable bond lengths and angles. The anion corresponding to the major component (**B**) is shown in Figure 1a. As can be observed, the anion is formed by two $Pt(C{\equiv}CTol)_4$ dianionic fragments bonded to a dicationic "$Pb(OH_2)_2$" unit. The anion exhibits a trigonal bipyramid coordination around the lead center with the platinum atoms defining the axial positions and the aqua ligands the equatorial positions, the third equatorial position being defined by the stereochemically active $6s^2$ lone pair[123,124] (Figure 1b). It should be noted that the coordination of water to lead is rare, and most of the structures reported contain only a single aqua ligand. Only a few crystallographic examples have been reported with two lead-bound water molecules[123,125] or with a Pb(II) contacting two bridged aqua ligands.[126] In this anion the Pb−O lengths (2.439(10), 2.469(8) Å) fall within the range reported for Pb−O distances in complexes with H_2O ligands.[96,123,125,127] Of greatest interest are the Pt−Pb distances, the first determined for a non bridged angular Pt−Pb−Pt entity. The distances Pt(1)−Pb(1b) (2.9109(5) Å) and Pt(2)−Pb(1b) (2.8908(5) Å) are only slightly longer than the sum of the covalent radii (2.75 Å).[128] As commented above, relatively few examples containing Pt−Pb bonding are reported, but these distances are slightly longer than those found in the anionic trinuclear $(NBu_4)_2[\{Pt(C_6F_5)_4\}_2Pb]$ **5** (2.769(2), 2.793(2) Å)[97] or $[(C_6F_5)_3Pt(\mu\text{-}X)(\mu\text{-}Pb)Pt(C_6F_5)_3]^-$ (2.701(1)−2.729(1) Å)[99] systems containing $Pt^{II}-Pb^{II}$ bonds and in the cationic $[Pt_2(P_2Phen)_3Pb]^{2+}$ (P_2Phen = 2,9-bis(diphenylphosphine)-1,10-phenanthroline) (2.7469(6), 2.7325(6) Å) with a linear $Pt^0-Pb^{II}-Pt^0$ core.[93] However, the $Pt^{II}-Pb^{II}$ bonding in the anion of **1** is certainly more significant than the $Pt^{II}-Pb^{II}$ bonding in $[(CH_3CO_2)Pb(\text{crown-}P_2)Pt(CN)_2]^+$ (3.312(2) Å).[96] The Pt−Pb bonds are slightly displaced from the normal to the platinum basal atoms (20.2(2)° for Pb(1b)−Pt(1) and 11.7(2)° for Pb(1b)−Pt(2)) leading to a Pt−Pb−Pt bent entity (149.95(2)°). The displacement of both Pt atoms out to their respective basal $(C_\alpha)_4$ planes toward the Pb center is negligible [0.0061(2) Å for Pt(1) and 0.0196(2) Å for Pt(2)].

As shown in Figure 1b, which emphasizes the very strong *hemidirected* coordination sphere of lead with the presumed lone pair located toward the opposite side of the remaining Pb−ligand interactions, the displacement of Pb from the axial Pt atoms could suggest a certain degree of Pb−C(alkynyl) bonding. However the $Pb-C_\alpha$ distances range from 3.046(9) to 3.46(1) Å and are considered essentially nonbonding. Notwithstanding, we note that $Pb\cdots C(\eta^2\text{-arene})$ interactions ranging from 3.083(6) to 3.309 Å,[129,130] and even longer ones (~3.6 Å),[131] have been reported.

The formation of complex $(NBu_4)_2[\{Pt(C{\equiv}CTol)_4\}_2Pb(OH_2)_2]$ **1** without Pb−alkyne interactions and stabilized mainly by Pt−Pb bonds is remarkable. In fact, we have recently shown that $[Pt(C{\equiv}CTol)_4]^{2-}$ reacts with the isoelectronic Tl^I ion forming the hexanuclear cluster $[Pt_2Tl_4(C{\equiv}CTol)_8(acetone)_2]$ stabilized, in this case, by $Tl\cdots\eta$ (alkynyl) bonds and containing only $Pt\cdots Tl$ (3.567(5)−3.7204(4) Å) contacts.[112] Because for both $6s^2$ ions, Pb^{II} and Tl^I, the $M\cdots$(alkyne) interaction virtually lacks the back bonding component, we would have expected the σ alkyne$\cdots$M (Tl^I, Pb^{II}) component to be stronger or greater with Pb^{II}.

To investigate the chance of obtaining species containing Pb^{II}−alkyne interactions we explored neutralization reactions starting from two monoanionic benzoquinolate *bis*(alkynyl)-platinate(II) species $[Pt(bzq)(C{\equiv}CR)_2]^-$ (R = Ph, $C_6H_4-CF_3$-4) bearing different alkynyl substituents. As is shown in Scheme 1, treatment of a yellow solution of $(NBu_4)[Pt(bzq)(C{\equiv}CPh)_2]$ in acetone with $Pb(ClO_4)_2\cdot 3H_2O$ (0.5 equiv) results in the immediate precipitation of $[\{Pt(bzq)(C{\equiv}CPh)_2\}_2Pb]$ **2** as an orange solid in high yield (82%). The analogous reaction of $(NBu_4)[Pt(bzq)(C{\equiv}CC_6H_4-CF_3\text{-}4)_2]$, containing the less electron-donating $C_6H_4-CF_3$-4 substituent, gives a deep orange solution from which the related trinuclear product $[\{Pt(bzq)(C{\equiv}CC_6H_4-CF_3\text{-}4)_2\}_2Pb]$ **3** is isolated in very low yield (8.5%) by removal of the solvent and addition of CH_2Cl_2 in which **3** separates as an orange solid. Surprisingly, the adduct $(NBu_4)[\{Pt(bzq)(C{\equiv}CC_6H_4-CF_3\text{-}4)_2\}_2Pb(O_2ClO_2)]$ **4** precipitated from the filtrate in moderate yield (39%) as a yellow microcrystalline solid. It should be noted that the color of **4** changed to orange immediately after drying. The neutral derivative $[\{Pt(bzq)(C{\equiv}CC_6H_4-CF_3\text{-}4)_2\}_2Pb]$ **3** can be obtained in higher yield

(123) Shimoni-Liuny, L.; Glusker, J. P.; Bock, C. W. *Inorg. Chem.* **1998**, *37*, 1853; and references therein.
(124) Briand, G. G.; Smith, A. D.; Schatte, G.; Rossini, A. J.; Schurko, R. W. *Inorg. Chem.* **2007**, *46*, 8625.
(125) Janiak, C.; Temizdemir, S.; Scharmann, T. G.; Schmalstieg, A.; Demtschuk, J. *Z. Anorg. Allg. Chem.* **2000**, *626*, 2053.
(126) Katz, M. J.; Aguiar, P. M.; Batchelor, R. J.; Bokov, A. A.; Ye, Z. G.; Kroeker, S.; Leznoff, D. B. *J. Am. Chem. Soc.* **2006**, *128*, 3669.
(127) Zhao, J. A.; Wang, Y. L.; Wang, Y. T.; Fang, Y. T.; Hou, H. W. *Synth. React. Met.-Org. Nano Met. Chem.* **2007**, *37*, 109.
(128) Lee, J. D. *Concise Inorganic Chemistry*, 5th ed.; Blackwell Science: Cambridge, MA, 1996.
(129) Frank, W.; Wiltmer, F. G. *Chem.Ber./Recl.* **1997**, *130*, 1731.
(130) Labah, D.; Bohnen, F. M.; Herbst Irmer, R.; Phol, E.; Stalke, D.; Roesky, H. W. *Z. Anorg. Allg. Chem.* **1994**, *620*, 41.
(131) Harowfield, J M.; Maghaminia, S.; Soudi, A. A. *Inorg. Chem.* **2004**, *43*, 1810.

Scheme 2

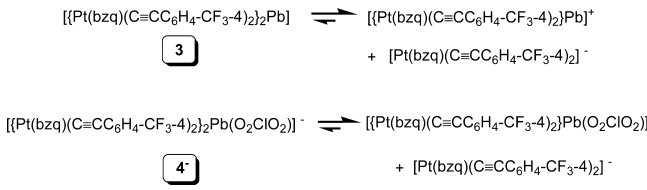

(79%) following similar work up but using excess of Pb^{II} (Pt:Pb 1:1) (see Experimental Section).

The IR spectrum of **2** exhibits a ν(C≡C) band at 2080 cm^{-1} with a shoulder at 2017 cm^{-1}. These values are lower than those observed in the precursor (2103, 2080 cm^{-1}),[37] suggesting that the lead center is probably π-interacting with the alkynyl fragments. Conductivity measurements (see Experimental Section) and the mass spectra (ES+), which exhibits the molecular peak (*m*/*z* 1359, 100%), indicate that the trinuclear entity remains in solution. The ^{1}H NMR spectrum at room temperature confirms the interaction of the Pb center with the platinum fragments. In particular, the resonances corresponding to H^2, H^9, and H^3 (see Scheme 1 for labeling), which were assigned by a ^{1}H−^{1}H COSY experiment, appear in the spectrum of **2** (δ ($CDCl_3$, ppm) 8.94 H^2; 8.39 H^9; 6.39 H^3) considerably shifted to lower frequencies in comparison with the precursor (δ ($CDCl_3$, ppm) 10.04 H^2; 8.56 H^9; 7.37 H^3). The characteristic ^{195}Pt coupling constants for H^2 and H^9 are, however, similar (30 and 42.5 Hz in **2** vs 23.6 and 40.0 Hz in $[Pt(bzq)(C{\equiv}CPh)_2]^-$). The ν(C≡C) bands in **3** and in the perchlorate adduct **4** appear at 2099, 2072 cm^{-1} (**3**) and at 2092, 2080 cm^{-1} (**4**). The most remarkable difference is the presence of two strong bands at 622 and 598 cm^{-1}, characteristic of the δ_{asym}(O−Cl−O) bending of the perchlorate group, which appear split, suggesting coordination of the perchlorate anion.[132] The typical bands at about 1090 cm^{-1} cannot be unambiguously assigned because of overlapping with bands of the C_6H_4−CF_3−4 substituents. Conductivity measurements of **3** in acetone (153 $\Omega^{-1}\cdot cm^2\cdot mol^{-1}$) indicate considerable dissociation of this product in solution. For the adduct **4**, the value obtained in acetone is 100.3 $\Omega^{-1}\cdot cm^2\cdot mol^{-1}$. The ^{1}H NMR spectra of **3** and **4** (CD_3COCD_3) are identical except for the presence of the signals corresponding to the NBu_4^+ cation in **4**. The remarkable displacement of the H^2, H^9, and H^8 signals in the proton spectra in CD_3COCD_3 (δ(ppm) 9.07 H^2; 8.33 H^9; 6.70 H^8) in relation to the precursor (10.1 H^2; 8.54 H^9; 7.53 H^8)[37] supports the presence of platinum−lead bimetallic fragments in solution. The addition of small amounts of the platinate precursor to these solutions causes the gradual shift of these signals to those seen for the precursor, indicating the presence, in acetone solution, of possible fast dissociative patterns as indicated in Scheme 2.

The structure of the neutral complex $[\{Pt(bzq)(C{\equiv}CPh)_2\}_2Pb]$ **2** and the perchlorate adduct $(NBu_4)[\{Pt(bzq)(C{\equiv}CC_6H_4{-}CF_3{-}4)_2\}_2Pb(O_2ClO_2)]$ **4** have been confirmed by X-ray crystallographic studies (Figures 2, 3; Tables 1, 2). The molecular structure of complex **2** (Figure 2a) can be described as two eclipsed (and *trans*-oriented) *bis*(alkynyl)-platinate(II) fragments connected by a Pb^{II} cation. The anionic motif of the adduct **4**, shown in Figure 3, is quite similar, the most surprising feature being the presence of a perchlorate anion, which is located close to the lead cation. In this anion, examination of the ΔMSDA values for the Pt−N and Pt−C_{orth} bonds of the Pt-bzq fragments suggests that both situations, *trans* and *cis*-oriented, are crystallographically present (50/50).

In the neutral complex **2** the intermetallic distances are only slightly asymmetric (Pt(1)−Pb(1) = 2.9759(5); Pt(2)−Pb(1) = 2.9182(5) Å) and comparable to those found in **1**, whereas they are rather asymmetric in the anion $\mathbf{4}^-$ (Pt(1)−Pb(1) = 2.8715(5) and Pt(2)−Pb(1) = 3.3136(5) Å). In both complexes the Pt(1)−Pb(1)−Pt(2) angle is very acute (74.782(14)° **2**; 75.873(13)° $\mathbf{4}^-$) with the Pb(1) leaning to the alkynyl entities. As a consequence the lead ion is therefore bonded to both platinum centers and the four available alkynyl fragments. In both derivatives the coordination to the $C_\alpha{\equiv}C_\beta$ bonds is unsymmetrical and mainly with the C_α carbon atoms. Thus, in the neutral complex **2**, the Pb−C_α distances (range 2.619(9) to 2.682(9) Å) are below the sum of the van der Waals radii of carbon (1.43 Å) and the covalent radii of lead (1.47 Å) (2.90 Å),[128] which is consistent with the existence of a weak coordinative interaction between Pb^{II} and the internal carbon atoms of the alkynyl entities. Although comparison is not easy, these values (2.619(9)−2.682(9) Å) are only slightly larger than the Pb^{IV}−C_α bond distance of 2.467(6) Å found in the zwitterionic complex $[^iPr_2B^-(C(^iPr){=}CMe)(\mu\text{-}C{\equiv}CMe)Pt^+Me_2]$,[114] taking into account the smaller size of the Pb^{IV} center. In this Pb^{IV} derivative the Pb−C_β distance was found to be 2.648(8) Å.[114] By contrast, in the trinuclear complex **2** the distances between the lead center and the external C_β carbon atoms are significantly larger by 0.35−0.57 Å (range of 3.00−3.22 Å) to the respective Pb−C_α distances, indicating that the interaction to these atoms is essentially negligible. It has been previously shown[133–135] that the Pb^{II} cation exhibits a very rich structural diversity with variable coordination numbers and geometries, which are modulated by the nature of the ligands and, additionally, by the stereochemical activity of the lone pair.[123,124,136–138] However, as has been previously noted,[131] in many complexes lead−donor atom distances are widely spread, generating some arbitrariness in the identification of the donor atoms and hence in the exact nature of the Pb coordination sphere and its geometry. In complex **2**, the bonding of Pb^{II} with the platina-alkynyl entities, Pt−$C_\alpha{\equiv}C_\beta$−Ph, could be con-

(132) Hathaway, B. J.; Underhill, A. E. *Chem. Soc.* **1961**, 3091.

(133) Claudio, E. S.; Godwin, H. A.; Magyar, J. S. *Prog. Inorg. Chem.* **2003**, *51*, 1.

(134) Parr, J. In *Comprehensive Coordination Chemistry II*; McCleverty, J., Meyer, T. J., Eds.; Pergamon: Oxford, 2003; Vol. *3*, pp 545−608.

(135) Sigel, H.; Da Costa, C. P.; Martin, R. B. *Coord. Chem. Rev.* **2001**, *219*, 436.

(136) Esteban-Gómez, D.; Platas-Iglesias, C.; Enríquez-Pérez, T.; Avecilla, F.; de Blas, A.; Rodríguez-Blas, T. *Inorg. Chem.* **2006**, *45*, 5407; and references therein.

(137) Noshiranzadeh, N.; Ramanzani, A.; Morsali, A.; Hunter, A. D.; Zeller, M. *Inorg. Chem. Commun.* **2007**, *10*, 738; and references therein.

(138) Esteban-Gómez, D.; Platas-Iglesias, C.; Avecilla, F.; de.Blas, A.; Rodríguez-Blas, T. *Eur. J. Inorg. Chem.* **2007**, 1635.

sidered to take place mainly with the Pt−C_α bonds; the Pb^{II} ion is therefore in an approximately square pyramidal geometry with the midpoint of the four Pt−C_α bonds occupying the basal plane, and the stereochemically active lone pair occupies the obvious gap in the metal ion coordination sphere at the apex of the pyramid. This geometry is consistent with the preferred *hemidirected* coordination observed for lead(II) compounds with low coordination numbers (2−5).

In the anion $\mathbf{4}^-$ (Figure 3) the interaction of the Pb^{II} ion with the C_α carbon atoms is unsymmetrical in such a way that the shorter Pb−C_α distances correlate with the longer Pb(1)−Pt one: Pb(1)−C(32) = 2.630(9); Pb(1)−C(41) = 2.659(10); Pb(1)−Pt(2) = 3.3136(5) Å versus Pb(1)−C(1) = 2.731(9); Pb(1)−C(10) = 2.772(10); Pb(1)−Pt(1) = 2.8715(5) Å. The distances to the external C_β atoms follow a similar tendency ranging from 2.94 to 3.33 Å. Both the platinum−lead and lead−alkynyl bond distances in **2** and $\mathbf{4}^-$ indicate that the interactions of the Pb^{II} ion are weaker with the $[Pt(bzq)(C{\equiv}CC_6H_4{-}CF_3\text{-}4)_2]^-$ entities, presumably because of the electron poor nature of the $C_6H_4-CF_3$-4 alkynyl substituents. As is shown in Figure 3, this fact appears to have an important effect on the final environment of the Pb^{II} ion, forcing it to come into contact with two oxygen atoms of a perchlorate group. The interaction between the Pb^{II} ion and this perchlorate is also unsymmetrical and very weak, as indicated by the Pb−O distances (Pb(1)−O(1) = 2.880(8) Å; Pb(1)−O(2) = 3.013(8) Å), but clearly contributes to fulfilling the requirements of the acidic Pb^{II} center. Similar long Pb^{II}−O contacts have been previously observed[138,139] and very often have been described as "semicoordination". Because of the unsymmetrical coordination of both platinate entities and that of the weakly bonded chelated perchlorate anion, the Pb center is in a more complicated environment (see inset in Figure 3) formed by the four Pt−C_α bonds and the two oxygen atoms. The low symmetry suggests that the Pb^{II} lone pair is still stereochemically active in the anion $\mathbf{4}^-$.

A remarkable feature in both structures is the close intramolecular separation between the square-planar platinate fragments. In complex **2** the benzoquinolate ligands are essentially eclipsed and both the interplanar spacing (3.36−3.48 Å) and the resulting Pt···Pt separation (3.5794(5) Å) are in the known range of $\pi\cdots\pi$ and Pt···Pt stacked interactions.[15,39,115,140–148] These short distances clearly contribute to the stability of the assembly. Further examination of the crystal packing of **2** reveals that the trinuclear clusters are additionally arranged in a head-to-tail orientation, giving rise to π-stacked dimers (3.36−3.42 Å) (Figure 2b). In the anion $\mathbf{4}^-$, the platinum planes are also π-interacting (3.20−3.61 Å), but they are slightly displaced (ca. 1.4 Å) and therefore the Pt···Pt separation increases to 3.8185(5) Å. This value is significantly longer than the usual range (3.0−3.5 Å) reported for dimers, oligomers, or even infinite columnar stacked Pt···Pt systems,[39,45] indicating no significant Pt−Pt interaction within the trinuclear anion.

Spectroscopic Studies. As noted in the Introduction, very few spectroscopic investigations have been reported for systems containing M···Pb^{II} bonds.[93–95,98–101] To gain further insight into the excited-state properties of complexes containing Pt−Pb(II) bonds, as well as to understand the influence of the stereochemical activity of the $6s^2$ lone pair on their photophysical properties, we have examined the behavior of **1**−**4**, which have angular Pt_2Pb entities, and of $(NBu_4)_2[\{Pt(C_6F_5)_4\}_2Pb]$ **5**, which exhibits a linear Pt−Pb−Pt unit and a clear *holodirected* geometry at Pb. The photophysical data of all complexes are collected in Table 3. The bonding associated to the trinuclear linear Pt(II)−Pb(II)−Pt(II) entity in the pentafluorophenyl derivative complex **5** can be rationalized using a simplified molecular orbital approach discussed elsewhere,[78,91,93,100] which has been supported by theoretical calculations on d^8-Tl-d^8 systems.[76,149] This involves the interaction between the filled $5d_{z^2}$ (2Pt) and 6s (Pb^{II}) orbitals and the empty set of $6p_z$ orbitals of the three (2Pt, Pb^{II}) metal centers. Mixing between levels stabilizes the filled orbitals relative to their unfilled counterparts, thereby giving the trinuclear unit stability. The solid state diffuse-reflectance and electronic absorption (CH_2Cl_2 10^{-4} M) UV−vis spectra of complex **5**, together with that of the precursor $(NBu_4)_2[Pt(C_6F_5)_4]$ for comparison, are shown in Figure 4. As can be seen, the two low energy features at 415 and 502 nm, observed in solid state, are also present in solution (408, 500 nm), confirming the integrity of the complex in CH_2Cl_2 solvent in agreement with previously reported NMR data.[97] In both media the intense absorption (408 nm, $\varepsilon = 16.3 \times 10^3$ M^{-1} cm^{-1}, CH_2Cl_2), absent in the precursor, is assigned to the spin-allowed $\sigma^*\rightarrow\sigma$ transition having a remarkable $Pt(5d_{z^2})\rightarrow Pb(6p_z)$ charge-transfer character (MM′CT).[76] The weaker feature, seen at lower energies (ca. 500 nm, $\varepsilon = 660$ M^{-1} cm^{-1}), is tentatively attributed to the direct population of the corresponding spin-forbidden $^3(\sigma^*\sigma)$ state. The high energy band at 232 nm is associated with IL $\pi\pi^*$ transitions on the C_6F_5 groups, although overlapping with sp metal centered transitions due to the lead(II) ion is quite likely. In fact, a solution of $Pb(ClO_4)_2$ in acetonitrile exhibits one band (242 nm, $\varepsilon = 763$ M^{-1} cm^{-1}) in this region (204, 242, 300 nm). The additional intense absorption at 320 nm ($\varepsilon = 25.5 \times 10^3$ M^{-1} cm^{-1}) observed

(139) Andersen, R. J.; diTargiani, R. C.; Hancock, R. D.; Stern, C. L.; Goldberg, D. P.; Godwin, H. A. *Inorg. Chem.* **2006**, *45*, 6574.
(140) Houlding, V. H.; Miskoswski, V. M. *Coord. Chem. Rev.* **1991**, *111*, 145.
(141) Connick, W. B.; Marsh, R. E.; Schaefer, W. P.; Gray, H. B. *Inorg. Chem.* **1997**, *36*, 913; and references therein.
(142) Connick, W. B.; Geiger, D.; Eisenberg, R. *Inorg. Chem.* **1999**, *38*, 3264.
(143) Buss, C. E.; Mann, K. R. *J. Am. Chem. Soc.* **2002**, *124*, 1031.
(144) Wadas, T. J.; Wang, Q. M.; Kim, K. Y.; Flaschenreim, C.; Blanton, T. N.; Eisenberg, R. *J. Am. Chem. Soc.* **2004**, *126*, 16841.
(145) Kui, S. C. F.; Chui, S. S. Y.; Che, C. M.; Zhu, N. *J. Am. Chem. Soc.* **2006**, *128*, 8297.
(146) Sun, Y. H.; Ye, K. Q.; Zhang, H. Y.; Zhang, J. H.; Zhao, L.; Li, B.; Yang, G. D.; Yang, B.; Wang, Y.; Lai, S. W.; Che, C. M. *Angew. Chem., Int. Ed.* **2006**, *45*, 5610; and references therein.
(147) Forniés, J.; Ibáñez, S.; Martín, A.; Sanz, M.; Berenguer, J. R.; Lalinde, E.; Torroba, J. *Organometallics* **2006**, *25*, 4331; and references therein.
(148) Kato, M. *Bull. Chem. Soc. Jpn.* **2007**, *80*, 287; and references therein.
(149) Dolg, M.; Pyykkö, P.; Runember, N. *Inorg. Chem.* **1996**, *35*, 7450.

Table 3. Photophysical Data for Complexes **1**−**5**

compound	medium (*T*/K)	absorption/nm (10^3 ε/M^{-1} cm^{-1})	λ_{em}^{max}/nm {τ [μs]}
1	solid (298)	270−400	non emissive
	solid (77)		497_{max} (λ_{ex} 295−460) [10]
	solid with acetone (298)		490_{max} (λ_{ex} 300−450) [14]
	solid with acetone (77)		478_{max} (λ_{ex} 300−447) [18]
	CH_2Cl_2 5×10^{-5} M (298)	270 (108.3), 435 (14.6)	non emissive
	CH_2Cl_2 5×10^{-5} M (77)		456_{max}, 500sh (λ_{ex} 300−377)
	acetone 5×10^{-5} M (298)		non emissive
	acetone 5×10^{-5} M (77)		490_{max}, 500sh (λ_{ex} 300−410)
2	solid (298)		non emissive
	solid (77)		607_{max} (λ_{ex} 300−500) [24]
	CH_2Cl_2 10^{-3} M (298)		non emissive
	CH_2Cl_2 10^{-3} M (77)		590_{max}, 648sh (λ_{ex} 400−540)
	CH_2Cl_2 5×10^{-5} M (298)	241 (68.3), 276 (58.8), 327sh (35.3), 430 (12.7)[a]	575_{max} (λ_{ex} 390)
	CH_2Cl_2 5×10^{-5} M (77)		490, 525, 582_{max} (λ_{ex} 450)
3	solid (298)		non emissive
	solid (77)		620_{max}, 660sh (λ_{ex} 450) [11(620)]
			620sh, 660_{max} (λ_{ex} 500) [12(660)]
	CH_2Cl_2[b]	233, 267, 280, 325sh, 425	
4	solid (298)		non emissive
	solid (77)		600_{max} (λ_{ex} 520) [18]
	CH_2Cl_2 5×10^{-5} M (298)	220 (121), 240sh (94.5), 290 (72.9), 393sh (13.1), ∼435sh (8.8)	non emissive
	CH_2Cl_2 5×10^{-5} M (77)		575_{max}, 660 (λ_{ex} 500) 575, 660_{max} (λ_{ex} 530)
5	solid (298)[c]	325, 415, 502	539_{max} (λ_{ex} 300−502) [9]
	solid (77)		529_{max} (λ_{ex} 300−490) [35]
	CH_2Cl_2 1.6×10^{-5} M (298)	232 (21.0), 320 (25.5), 408 (16.3), 500 (0.66)	
	CH_2Cl_2 4×10^{-4} M (298)[d]		533_{max} (λ_{ex} 300−498) [11]
	CH_2Cl_2 4×10^{-4} M (77)		520_{max} (λ_{ex} 317−495) [113]
	2-MeTHF 4×10^{-4} M (298)[e]		533_{max} (λ_{ex} 300−498)
	2-MeTHF 4×10^{-4} M (77)		520_{max} (λ_{ex} 317−495)

[a] Similar absorption spectra were obtained at 10^{-4}, 5×10^{-4} and 10^{-3} M. [b] The low solubility of this complex precludes the determination of the ε values with accuracy. [c] $\phi = 0.43$. [d] $\phi = 4.5 \times 10^{-3}$. [e] $\phi = 6.4 \times 10^{-4}$.

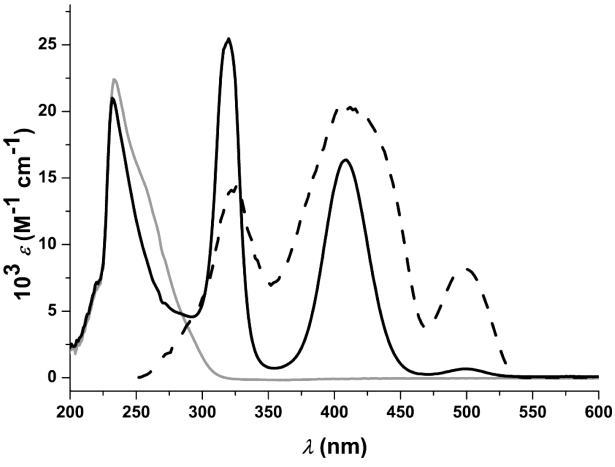

Figure 4. Absorption spectra of **5** (dark solid line) and complex $(NBu_4)_2[Pt(C_6F_5)_4]$ (light solid line) in CH_2Cl_2 10^{-4} M and reflectance diffuse (dashed line) of **5** (a.u.).

in complex **5** could be associated tentatively mainly with a spin-allowed sp metal (Pb^{II}) centered transition.

The angular trinuclear complex $(NBu_4)_2[\{Pt(C{\equiv}CTol)_4\}_2Pb(OH_2)_2]$ **1** shows in solution a strong band at 270 nm and an extended low energy feature from ∼350 to 450 nm, this latter being absent in the precursor ($(NBu_4)_2[Pt(C{\equiv}CTol)_4]$ 285, 334, 345(sh), CH_2Cl_2), which can be related to the presence of Pt−Pb bonds. Both neutral derivatives [{Pt(bzq)(C≡CR)$_2$}$_2$Pb] (R = Ph **2**; R = C_6H_4−CF_3-4 **3**) (Supporting Information, Figures S1 and S2), having Pb···alkynyl and Pt···Pb bonding interactions, exhibit in CH_2Cl_2 solution high-energy intraligand (bzq, C≡CR) absorptions and a low energy band (430 nm **2**; 425 nm **3**) that is notably red-shifted in relation to the corresponding precursors (R = Ph 397 nm; R = C_6H_4−CF_3−4 392 nm).[37] On the basis of previous assignments made in related heteropolymetal η-alkynyl bridging complexes,[39–42,51,107,108] this absorption is tentatively assigned to an admixture of platinum-perturbed intraligand IL ($\pi{\rightarrow}\pi^*$ C≡CAr) and LM′CT [alkynyl or platina-alkynyl-M′(Pb) charge transfer Pt−C≡CAr→6s/p(Pb)] modified by $Pt^{II}{\cdots}Pb^{II}$ interactions. The small blue shift from **2** to **3** (∼5 nm, 274 cm^{-1}) is consistent with the lesser donor capability of the C≡CC_6H_4−CF_3-4 group to the lead(II) center. In contrast to the low solubility of complex **3** in CH_2Cl_2 (see bottom (b) of Table 3), the perchlorate adduct $(NBu_4)[\{Pt(bzq)(C{\equiv}CC_6H_4{-}CF_3\text{-}4)_2\}_2Pb(O_2ClO_2)]$ **4** is very soluble, and the most significant difference with the absorption spectrum of complex **3** is the occurrence of two low features at about 393 and 435 nm. The band at 393 nm is believed to be due to the presence of the anionic precursor fragment $[Pt(bzq)(C{\equiv}CC_6H_4{-}CF_3\text{-}4)_2]^-$ in solution. This fact, in agreement with the NMR data, suggests that its integrity is at least partially broken in solution, presumably favored by the presence of the perchlorate group, which competes with the platinate $[Pt(bzq)(C{\equiv}CC_6H_4{-}CF_3\text{-}4)_2]^-$ (Scheme 2).

The linear pentafluorophenyl platinate-lead complex $(NBu_4)_2[\{Pt(C_6F_5)_4\}_2Pb]$ **5** exhibits (Figure 5) a bright, long-lived (τ = 9 μs) green luminescence in solid state at room temperature (λ_{em} 539 nm, ϕ = 0.43, λ_{exc} = 450 nm) by excitation in the 300−502 nm range, which is slightly blue-shifted (529 nm, τ = 35 μs) at 77 K. As can be observed in Figure 5, a similar long-lived emission is observed in solution

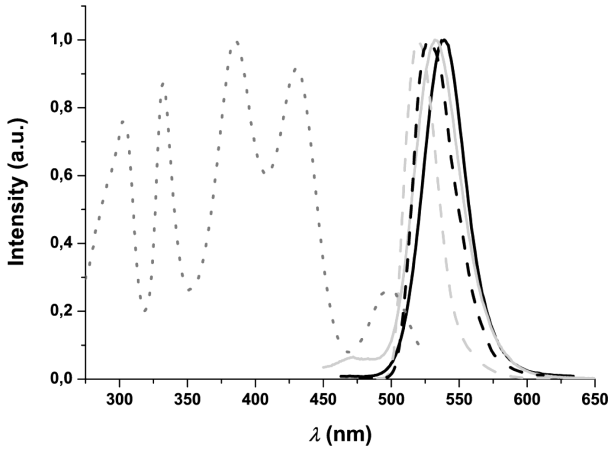

Figure 5. Normalized emission and excitation spectra of **5**: (dark solid line) solid at 298 K (λ_{exc} 300−502 nm); (dark dashed line) solid at 77 K (λ_{exc} 300−490 nm); (light solid line) CH_2Cl_2 (4×10^{-4} M) at 298 K (λ_{exc} 300−498 nm); (light dashed line) CH_2Cl_2 (4×10^{-4} M) at 77 K (λ_{exc} 317−495 nm); (light dotted line) CH_2Cl_2 (4×10^{-4} M) at 298 K (λ_{em} 533 nm).

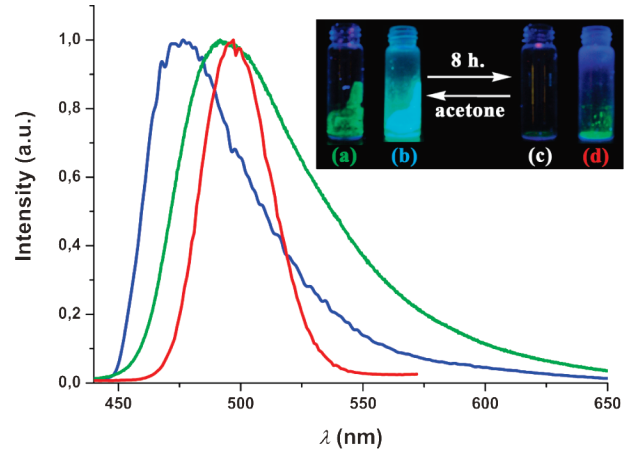

Figure 6. Normalized emission spectra of **1**: freshly solid at 298 K (green, a), or at 77 K (blue, b); the same sample after 8 h is not emissive at 298 K (c), but it is at 77 K (red, d).

either in a nondonor solvent such as dichloromethane ($\phi = 4.5 \times 10^{-3}$) or in 2-MeTHF ($\phi = 6.4 \times 10^{-4}$) at room temperature (533 nm, λ_{exc} 300−498 nm, $\tau = 11$ μs in CH_2Cl_2). When the solution is frozen at 77 K, the emission considerably increases its lifetime (113 μs in CH_2Cl_2 glass) and is again shifted to high energies (λ_{em} 520 nm, CH_2Cl_2, 2-MeTHF). Similar *rigidochromism* has been previously observed in other polynuclear complexes,[40,42,150] and could be ascribed to the minor structural changes that are accessible in the rigid matrix in relation to the solution. The excitation spectra, both in rigid media (solid, glass) and in solution (see Figure 5), are parallel to their corresponding absorption spectra (Figure 4) (CH_2Cl_2, solid). The emission in solid state can be compared to that observed in the isoelectronic $Pt^{II}-Tl^{I}-Pt^{II}$ complex $(NBu_4)_3[\{Pt(C_6F_5)_4\}_2Tl]$ (450 nm, 298 K; 445 nm, 77 K)[78] or in $[Tl_2Pt(CN)_4]$ (448 nm),[105] which have been attributed to a metal-centered phosphorescence process ($Pt(5d_{z^2}) \rightarrow Tl(6p_z)$) associated to the trinuclear entities (M−M′−M). The remarkable red-shift observed in $(NBu_4)_2[\{Pt(C_6F_5)_4\}_2Pb]$ **5** (539 nm, 298 K) is coherent with the presence of shorter Pt−Pb bond distances: 2.769(2), 2.793(2) Å in **5** versus 2.9777(4), 3.0434(4) in $(NBu_4)_3[\{Pt(C_6F_5)_4\}_2Tl]$[78] or 3.140(1) Å in $Tl_2[Pt(CN)_4]$.[105]

As commented above, complex **1** precipitates in acetone as a lemon-yellow solid, that exhibits a green luminescence visible to the naked eye under excitation using a conventional UV-lamp. However, when the solid is filtered, the initial luminescence observed at 490 upon exciting in the 300−450 nm range (Figure 6) and with a lifetime of triplet multiplicity (~14 μs) gradually decreases. In about 8 h, the color of the solid changes to pale yellow, and the final complex **1** does not exhibit luminescence at room temperature. The process is reversible, and the color and luminescence is recovered upon exposure of the aged solid to a drop of acetone. As can be observed in Figure 6, both solids are emissive at 77 K, and the most significant difference is that the solid exposed to acetone gives the maximum shifted to the blue (478 nm vs 497 nm **1**) and has a longer lifetime (18 vs 10 μs **1**). Despite many attempts, we were not successful in obtaining suitable crystals for an X-ray study from acetone solutions, and thus, the effect of the acetone on the structure and its influence on the final luminescence is not exactly known. The initial solid exhibits in its IR spectrum a ν(C═O) at 1720 cm^{-1} because of the presence of acetone, and the signal due to H_2O (~3375 br) is barely seen. By contrast, when the color of the solid has changed to pale yellow, the broad band at 3375 cm^{-1} is clearly seen while the acetone is lost. We think that the change in the color of the complex and the quenching of luminescence at room temperature is likely due to the fact that the initial solid has one or two acetone molecules weakly bonded to the lead center, which in the presence of air are replaced by H_2O giving rise to the final complex **1**. As in complex **5** the nature of the emission is suggested to be phosphorescence of the $^3(d\sigma^*p\sigma)$ excited state, related to the bent trinuclear Pt−Pb−Pt entity. The remarkable blue shift observed in the solid **1** at 77 K (497 nm) in comparison to **5** (529 nm) is in accordance with the presence of weaker Pt−Pb bond distances (2.9109(5), 2.8908(5) Å **1** vs 2.769(2), 2.793(2) Å **5**). In contrast to **5**, fluid solutions of **1** in CH_2Cl_2 or acetone are not emissive, probably because of the lesser rigidity of the bent Pt−Pb−Pt unit, which favors radiationless deactivation. Upon freezing to 77 K the behavior of both solutions is different. Thus, whereas the acetone solution glass produces a similar green emission (490 nm) to that seen in solid state, a high-energy bluish emission (456, 500sh nm) is observed in CH_2Cl_2 at 77 K. This emission is comparable to that of the homoleptic precursor $((NBu_4)_2[Pt(C{\equiv}CTol)_4]$ λ_{max} 456, 480, 502, 530 nm) and is thus attributed to an $^3IL(\pi\pi^*)/^3MLCT$ excited state.

The trinuclear benzoquinolate derivatives **2**−**4** are non emissive in solid state at room temperature, whereas both precursors $(NBu_4)[Pt(bzq)(C{\equiv}CR)_2]$ (R = Ph, $C_6H_4-CF_3$-4) were reported to exhibit long-lived, intense, structured emissions attributed to a metal perturbed L′LCT $^3[Pt(d)/\pi(C{\equiv}CR) \rightarrow \pi^*(bzq)]$ excited state.[37] The reason for the quenching of the luminescence is unclear, though we have found similar behavior in other polymetallic Pt−Cd[109] and

(150) Ford, P. C.; Cariati, E.; Bourassa, J. *Chem. Rev.* **1999**, *99*, 3625.

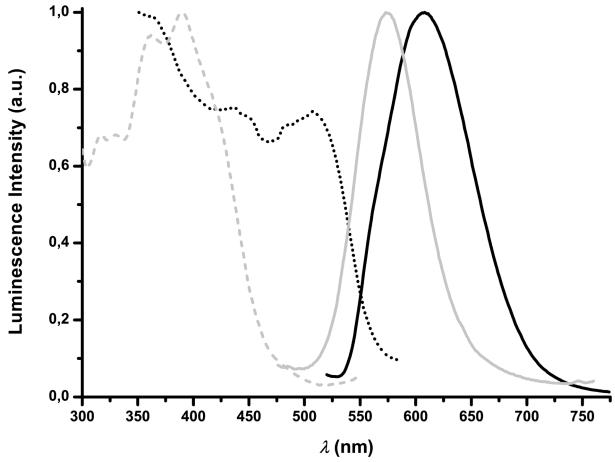

Figure 7. Normalized emission and excitation spectra of **2**: solid at 77 K, (dark solid line) λ_{exc} 500 nm, (dark dotted line) λ_{em} 607 nm; CH_2Cl_2 5 × 10^{-5} M at 298 K, (light solid line) λ_{exc} 390 nm, (light dashed line) λ_{em} 570 nm.

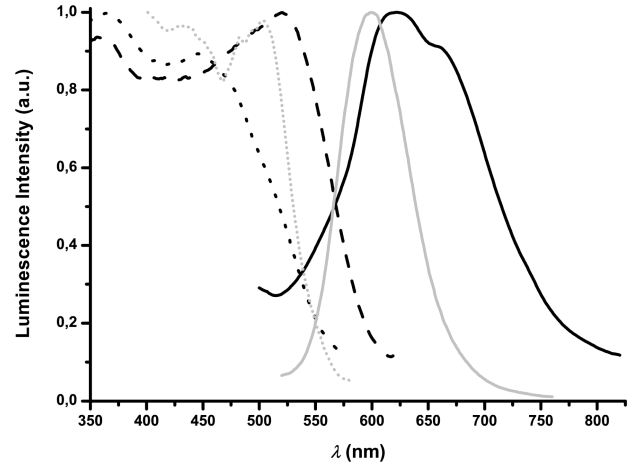

Figure 8. Normalized emission and excitation spectra of **3** and **4** in solid state at 77 K: **3** (dark solid line) λ_{exc} 450 nm, (dark dotted line) λ_{em} 620 nm, (dark dashed line) λ_{em} 660 nm; **4** (light solid line) λ_{exc} 520 nm, (light dotted line) λ_{em} 600 nm.

Pt−Au[40] complexes. However, upon cooling to 77 K all three complexes **2**−**4** exhibit long-lived, intense emissions (see Table 3). Complex **2** produces a bright orange emission (λ_{max} at 607 nm, 24 μs, λ_{ex} 300−500 nm), which is remarkably blue-shifted in a fluid dilute CH_2Cl_2 solution (λ_{max} 575 nm) by approximately 920 cm^{-1} (Figure 7). The emission is related to an excitation profile with several maxima (360, 390, ∼430sh nm) in the 320−450 nm range. The assignment of the radiative excitation state in solution is uncertain because of the presence of not only Pt···Pb but also Pb···η(C≡C) alkynyl and Pt···Pt bonding in the trinuclear entity. In this case, the remarkable red shift observed in CH_2Cl_2 solution in relation to the emission in the linear trinuclear derivative $(NBu_4)_2[\{Pt(C_6F_5)_4\}_2Pb]$ **5** (533 nm), with stronger Pt−Pb bonds, suggests that the emission in **2** could be related to the presence of Pb···η(C≡C) alkynyl interactions, though the influence of metal···metal bonding can not be discarded. Considering this and also the previous work on heteropolynuclear alkynyl bridging Pt^{II}−M complexes, the emissive state is likely to derive from a ^{3}MLM′CT [Pt(d)/π(C≡CPh)→Pt(p_z)/Pb(sp)/π*(C≡CPh)] state modified by metal···metal interactions in view of the short Pt···Pb and even Pt···Pt (3.5794(5) Å) separations.

Interestingly, the emission in solution is quenched by increasing the concentration to 10^{-3} M, probably because of the formation of dimers through intermolecular π···π (bzq) interactions as observed in solid state. Similar luminophore quenching due to π···π interactions between planar bzq ligands could be responsible for the lack of emission in solid state at 298 K. The emissions of the glasses are also concentration dependent (see Table 3). Thus, whereas a frozen concentrated (10^{-3} M) solution only displays a low energy emission (590, 648(sh) nm), which is independent of the excitation wavelength (400−540 nm), upon dilution (5 × 10^{-5} M) an additional, structured, high-energy band appears (490, 525sh). The high energy structured feature with vibrational spacing of 1360 cm^{-1} is suggestive of a substantial ^{3}MLCT character. The excitation profile (Figure 7) of the observed low temperature (77 K) solid state emission at 607 nm differs from that of the fluid solution showing an extended feature with a sharp edge located at about 530 nm, suggesting a certain degree of solid state effect in the emissive manifold. Because of the presence of dimers through short π···π interactions, it may be possible that the excited-state derives from similar ^{3}MLM′CT [Pt(d)/π(C≡CPh)→Pt(p_z)/Pb(sp)/π*(C≡CPh)] transitions mixed with some $\pi\pi$* excimeric character.

Figure 8 shows both emission and excitation spectra of $[\{Pt(bzq)(C{\equiv}CC_6H_4{-}CF_3\text{-}4)_2\}_2Pb]$ **3** and $(NBu_4)[\{Pt(bzq)(C{\equiv}CC_6H_4{-}CF_3\text{-}4)_2\}_2Pb(O_2ClO_2)]$ **4** in solid state at 77 K. As can be observed, complex **3** shows a broad profile with two maxima at 620 and 660 nm whose relative intensities depend on the excitation wavelength. Excitation profile monitoring at 620 and 660 nm is also different, suggesting the presence of different emissive states, presumably because of ground-state heterogeneity perhaps caused by the coexistence of monomers and π···π or Pt···Pt dimers in the crude solid. Compared to **2**, the remarkable red shift of these bands is in agreement with the involvement of the lower lying π*(C≡$CC_6H_4{-}CF_3$-4) orbitals (better accepting than π*(C≡CPh)) in the excited state. The weak coordination of the perchlorate anion to the lead center in the adduct **4** causes a significant shift to high energies (600 nm), and the band narrows considerably. This fact could be ascribed to the presence of Pb···O ($O_2ClO_2^-$) contacts, which presumably weaken the interaction of the lead center with the $C{\equiv}CC_6H_4{-}CF_3$-4 entities thus increasing the energy of the π*(C≡CAryl) based lowest unoccupied molecular orbital (LUMO). At 298 K, solutions of **3** (saturated) and **4** in CH_2Cl_2 do not exhibit luminescence. Upon cooling a dilute sample of **4** (5 × 10^{-5} M), the rigid glass shows a strong emission formed by two bands centered at 575 and 660 nm (Supporting Information, Figure S3). Its relative intensity is dependent on the excitation energy, and the excitation spectra are also different, indicating the presence of different emissive species. In fact, the excitation spectra monitored at 660 nm coincide with those of the low energy peak (660 nm) of solid **3** at 77 K, suggesting the formation of similar emissive species in the rigid glass.

Conclusions

In summary, we have prepared and characterized four novel trinuclear $Pt^{II}-Pb^{II}-Pt^{II}$ systems using homoleptic $[Pt(C{\equiv}CTol)_4]^{2-}$ and heteroleptic $[Pt(bzq)(C{\equiv}CR)_2]^-$ (R = Ph, $C_6H_4-CF_3$-4) anions as precursors. A comparison of the crystal structures of **1**, **2**, and **4** with that of previously reported $(NBu_4)_2[\{Pt(C_6F_5)_4\}_2Pb]$ **5** indicates that the local environment of Pb^{II} is highly sensitive to the nature of the anionic platinate precursor. Thus, whereas in the dianion $\mathbf{1}^{2-}$ the $6s^2$ lone pair of the Pb^{II} is stereochemically active, giving rise to a final trigonal bipyramidal coordination, with the Pt^{II} centers and the H_2O ligands defining the axial and the equatorial positions, respectively, in $[\{Pt(C_6F_5)_4\}_2Pb]^{2-}$ ($\mathbf{5}^{2-}$) it is inactive leading to a linear Pt−Pb−Pt entity with very short $Pt^{II}-Pb^{II}$ bond distances. It should be noted that, in spite of the well-known η^2-bonding capability of alkynyl groups, in this system the possible interaction with the Pb^{II} does not take place or is negligible. By using the heteroleptic fragments $[Pt(bzq)(C{\equiv}CR)_2]^-$ as metalloligands both the alkynyl ligands and the basic Pt^{II} center contribute to fulfilling the electronic requirements of the Pb^{II}, probably because of the lesser negative charge on the platinum centers. In the neutral derivative $[\{Pt(bzq)(C{\equiv}CPh)_2\}_2Pb]$ **2** (and probably in **3**) the lead center also shows a symmetric *hemidirected* coordination, being bonded to four $Pt-C_\alpha$ bonds, which define the basal plane of a square pyramidal geometry and have the lone pair at the apex of the pyramid. Because of the electron poor nature of the $C_6H_4-CF_3$-4, in the reaction mixture $[Pt(bzq)(C{\equiv}CC_6H_4-CF_3\text{-}4)_2]^-/Pb(ClO_4)_2$ (2:1) one of the perchlorate leaving groups contacts weakly, in a chelating way, with the Pb^{II}, forming the adduct $(NBu_4)[\{Pt(bzq)(C{\equiv}CC_6H_4-CF_3\text{-}4)_2\}_2Pb(O_2ClO_2)]$ **4**, in which the lead center presents a final unsymmetrical octacoordination.

In contrast to the linear derivative $(NBu_4)_2[\{Pt(C_6F_5)_4\}_2Pb]$ **5**, which exhibits a very strong luminescence both in solution (533 nm, ϕ 4.5 × 10^{-3} in CH_2Cl_2 and ϕ 6.4 × 10^{-4} in 2-MeTHF) and in solid state (539 nm, ϕ 0.43), probably because of its rigidity attributed to the Pt−Pb−Pt entity $^3[Pt(d_{z^2})\rightarrow Pb(6p_z)]$, complex **1** is only luminescent at low temperature (77 K, 497 nm solid; 478 nm glass). The lack of luminescence in solid state at room temperature of complex **1** could be attributed to the existence of an easy nonradiative relaxation due to the presence of the two lead bound to water molecules. Previous studies have shown that O−H oscillators in bound water molecules are very effective quenchers, both in solid state and in solution.[151] Notwithstanding, in solution the lesser rigidity of complex **1** due to the stereochemically active lone pair could also favors the radiationless deactivation. This behavior suggests that the metal-based phosphorescence (MM′CT) of the trinuclear $Pt^{II}-Pb^{II}-Pt^{II}$ cromophore is strongly influenced by the environment of the local center, being enhanced in more rigid holodirected coordination. Complexes **2**−**4** exhibit a yellow (**4**) or orange (**2**, **3**) emission in solid state at 77 K, tentatively assigned to a ^{3}MLM′CT $[Pt(d_{z^2})/\pi(C{\equiv}CR)\rightarrow Pt(p_z)Pb(sp)/\pi^*(C{\equiv}CR)]$ probably combined with some $\pi\pi^*$ excimeric character in neutral derivatives **2** and **3**, and in the case of adduct $(NBu_4)[\{Pt(bzq)(C{\equiv}CC_6H_4-CF_3\text{-}4)_2\}_2Pb(O_2ClO_2)]$ **4** modified by the presence of additional $Pb^{II}\cdots O$ ($O_2ClO_2^-$) contacts.

Acknowledgment. We thank the Ministerio de Ciencia y Tecnología (Project CTQ2005-08606-C02-01, 02 and grants for A.G. and A.D.). J.F. wishes to thank the CAR for a grant.

Supporting Information Available: Additional spectra of **2** and **3** and their corresponding precursors (UV, Figures S1, S2) and **4** (excitation and emission, Figure S3) (PDF). Crystallographic data in CIF format. This material is available free of charge via the Internet at http://pubs.acs.org.

IC8006876

(151) Beeby, A.; Clarkson, I. M.; Dickins, R. S.; Faulkner, S.; Parker, D.; Royle, L.; de.Sousa, A. S.; Williams, J. A. G.; Woods, M. *J. Chem. Soc., Perkin Trans 2* **1999**, 493.